Geochimica et Cosmochimica Acta 367 (2024) 72–86

Contents lists available at ScienceDirect

Geochimica et Cosmochimica Acta

journal homepage: www.elsevier.com/locate/gca

Chalcophile element degassing at an active continental arc volcano

Emily M. Mason [a], Marie Edmonds [a,*], Samantha Hammond [b], Evgenia Ilyinskaya [c], Frances Jenner [b], Barbara Kunz [b], Emma J. Nicholson [d], Gabriela Velasquez [e]

[a] Department of Earth Sciences, University of Cambridge, Cambridge, UK
[b] School of Environment, Earth and Ecosystem Sciences, Open University, Milton Keynes MK7 6AA, UK
[c] School of Earth and Environment, University of Leeds, Leeds, UK
[d] Department of Earth Sciences, University College London, London, UK
[e] Observatorio Volcanológico de los Andes del Sur (OVDAS), Red Nacional de Vigilancia Volcánica, Servicio Nacional de Geología y Minería, Temuco, Chile

ARTICLE INFO

Associate editor: Zoltan Zajacz

Keywords:
Chalcophile
Degassing
Subduction

ABSTRACT

Arc volcanoes are significant natural sources of trace chalcophile elements to the atmosphere via gas and aerosol plumes. Villarrica volcano, part of the Andean arc, erupts basaltic magmas and is characterised by a persistent volcanic gas plume and therefore presents an opportunity to quantify volcanic chalcophile processing in a subduction zone from slab to surface. Here we present geochemical data for olivine-hosted melt inclusions, as well as for the gas and aerosol plume. We show that melts erupted at Villarrica are enriched (over mid-ocean ridge basalts) in a suite of fluid-mobile elements comprising the large ion lithophiles, including Cs, and chalcophile elements W, Tl, Pb and Sb. Volcanic gas and aerosol samples show that the chalcophile elements, and Cs, are strongly enriched in the gas phase over the silicate melt, 10^3 to 10^6 times more so than the non-volatile Rare Earth Elements. Volatilities (the percentage of an element that degasses from a melt on eruption) reach ~ 45 % for Tl, with Pb, Sn and Mo exhibiting volatilities of up to 0.3 % and Cu up to 0.08 %. Many of the chalcophile elements (e.g. Cu, Ag, Zn) have an affinity for chloride in the gas phase and we observe that the volatility of chloride-speciating trace metals is linked strongly to the availability of chlorine in volcanic plumes globally. Overall, we show that the trace element composition of the volcanic gas—and hence probably also the deeper, denser and more saline fluids in the subsurface—is sensitive to both the availability of chloride in the gas phase and the composition of the melt, which is controlled by the slab flux and may be variable between subduction zones.

1. Introduction

Abundances of chalcophile elements in magmas are powerful tools to study magmatic processes such as differentiation, sulfide saturation and degassing (Jenner, 2017; Richards, 2015; Sillitoe, 2010; Zelenski et al., 2014). Many of the economically-important chalcophile elements are found in porphyry Cu-Au deposits that are associated with convergent margins (Lee and Tang, 2020; Sillitoe, 2010). Studies have shown that volcanic rocks in arc settings are enriched in the chalcophile elements lead (Pb), bismuth (Bi), tungsten (W), thallium (Tl), antimony (Sb) and arsenic (As) compared to mid-ocean ridge basalts (MORB), which suggests these elements are fluid-mobile during slab devolatilisation (Cox et al., 2019; Jenner, 2017; Noll Jr et al., 1996). Many chalcophile elements partition strongly into sulfides when magmas reach sulfide saturation (Kiseeva and Wood, 2013; Patten et al., 2013), which occurs as a function of magma temperature, pressure, oxygen fugacity and composition (Beermann et al., 2011; Jugo, 2009; O'Neill and Mavrogenes, 2022; Smythe et al., 2017). Global observations of copper (Cu) depletion in calc-alkaline, evolved arc volcanic rocks suggest that chalcophile elements may be sequestered in sulfide cumulates in the lower continental crust (Chen et al., 2020; Jenner, 2017).

At mid to low crustal pressures, magmas exsolve dense, saline aqueous fluid (Candela, 1997; Edmonds and Wallace, 2017; Hedenquist and Lowenstern, 1994). Chalcophile elements partition strongly into this aqueous fluid (Candela and Holland, 1984; Keppler and Wyllie, 1991; Williams-Jones and Heinrich, 2005; Zajacz et al., 2008), which unmixes into a brine and low density vapour at low pressures (Hedenquist and Lowenstern, 1994; Heinrich et al., 1999; Heinrich et al., 1992). Any disseminated sulfides present in the melt during degassing may break down and chalcophile elements may be transferred back into the

* Corresponding author.
E-mail address: marie.edmonds@esc.cam.ac.uk (M. Edmonds).

https://doi.org/10.1016/j.gca.2023.12.014
Received 25 April 2023; Accepted 12 December 2023
Available online 16 December 2023

melt-fluid system (Mungall et al., 2015; Reekie et al., 2019; Wieser et al., 2020).

Volcanoes emit gases into the atmosphere (Edmonds, 2021; Fischer and Chiodini, 2015; Symonds et al., 1994) in the form of plumes containing mixtures of water, carbon dioxide, sulfur and halogen gases and trace elements (including chalcophile elements), which form aerosol once in the atmosphere (Ilyinskaya et al., 2017; Mason et al., 2021; Mather et al., 2003). The extent to which chalcophile elements are degassed from silicate melt is described by their volatility, which can be quantified using emanation coefficients (Lambert et al., 1985). After degassing at the lava-air interface, volcanic gases cool rapidly and condense into fine particulate matter (Hinkley, 1991; Whitby, 1978). Volcanogenic gas and aerosol emissions have been sampled and studied at many volcanoes (Aiuppa et al., 2003; Allard et al., 2000; Allard et al., 2016; Buat-Ménard and Arnold, 1978; Gauthier et al., 2016; Hinkley et al., 1999; Ilyinskaya et al., 2017; Mandon et al., 2020; Mandon et al., 2019; Mason, 2021; Mather et al., 2012; Moune et al., 2010; Zelenski et al., 2021). Many volatile chalcophile elements are environmental pollutants that can be damaging to human health, e.g., As, Cd, Cu, Pb, Mo, Se, Tl, W and Zn (Stewart et al., 2022). During periods of intense unrest or eruption, volcanoes may be large point sources of elements such as Cd, Cu and Pb into the environment, at rates that may rival anthropogenic emissions from entire regions (e.g., the Mediterranean basin; Buat-Ménard & Arnold, 1978) or countries (Ilyinskaya et al., 2021).

Arc volcanic gases and aerosols exhibit enrichments in some chalcophile elements over volcanic gases and aerosols found in oceanic intraplate settings, such as W, Cs, As, Tl, Ag and Pb, whereas elements such as Se and Te may be more enriched in volcanic gas and aerosol in oceanic intraplate settings (Gauthier et al., 2016; Mason et al., 2021). These differences in volcanic gas composition between the two tectonic settings have been attributed to the combined effects of the hydrous nature of arc magmas, which causes fluid saturation at low melt fractions (Rezeau and Jagoutz, 2020), differences in the relative timing of aqueous fluid saturation versus sulfide saturation, and the higher salinity of the magmatic exsolved volatile phase in arc systems, which promotes the fluid-melt partitioning of species that speciate with chloride (Zelenski et al., 2021). In contrast, at oceanic intraplate volcanoes, lower magmatic water and chlorine contents suppress degassing of chalcophile metals until low pressures.

Volcán Villarrica (Chile), in the Andean arc (Fig. 1), is a typical stratovolcano located in the Southern Volcanic Zone (SVZ) of the Chilean Andes. Volcanic activity at Villarrica is characterised by persistent degassing from an open lava lake at the summit, with periodic Strombolian explosions and lava fountaining. Villarrica's most recent paroxysmal activity occurred in early 2015; the eruption was preceded by several weeks of unrest (Aiuppa et al., 2017; Johnson et al., 2018) that culminated in a 1.5 km-high lava fountain on 3 March 2015 (Romero et al., 2018). Erupted magma compositions range from basaltic to basaltic-andesite (50–57 wt% SiO_2) (Romero et al., 2018). Villarrica is a persistent source of gas and particulate matter emissions within the SVZ and has maintained an SO_2 flux on the order of a few hundred tons per day (t day^{-1}) during several campaign measurements since 2005 (Aiuppa et al., 2017; Liu et al., 2019; Moussallam et al., 2016; Palma et al., 2008; Sawyer et al., 2011; Witter et al., 2004) and by a permanent DOAS network since 2010 maintained by the Observatorio Volcanológico de los Andes del Sur (OVDAS). There have been numerous studies of the gas composition involving the major species (e.g., H_2O, SO_2, HCl) emitted from Villarrica (Aiuppa et al., 2017; Liu et al., 2019; Moussallam et al., 2016; Sawyer et al., 2011; Shinohara and Witter, 2005). Observed SO_2/HCl molar ratios ($\sim 2.3^{+0.7}_{-2.1}$) in gas emissions from Villarrica are typical of basaltic to basaltic-andesitic arc volcanoes (Aiuppa, 2009). Several studies at Villarrica have included characterisation of the particulate matter composition (Mather et al., 2004; Sawyer et al., 2011).

High concentrations of Cu (up to ~4800 ppm) and Ag (up to ~950

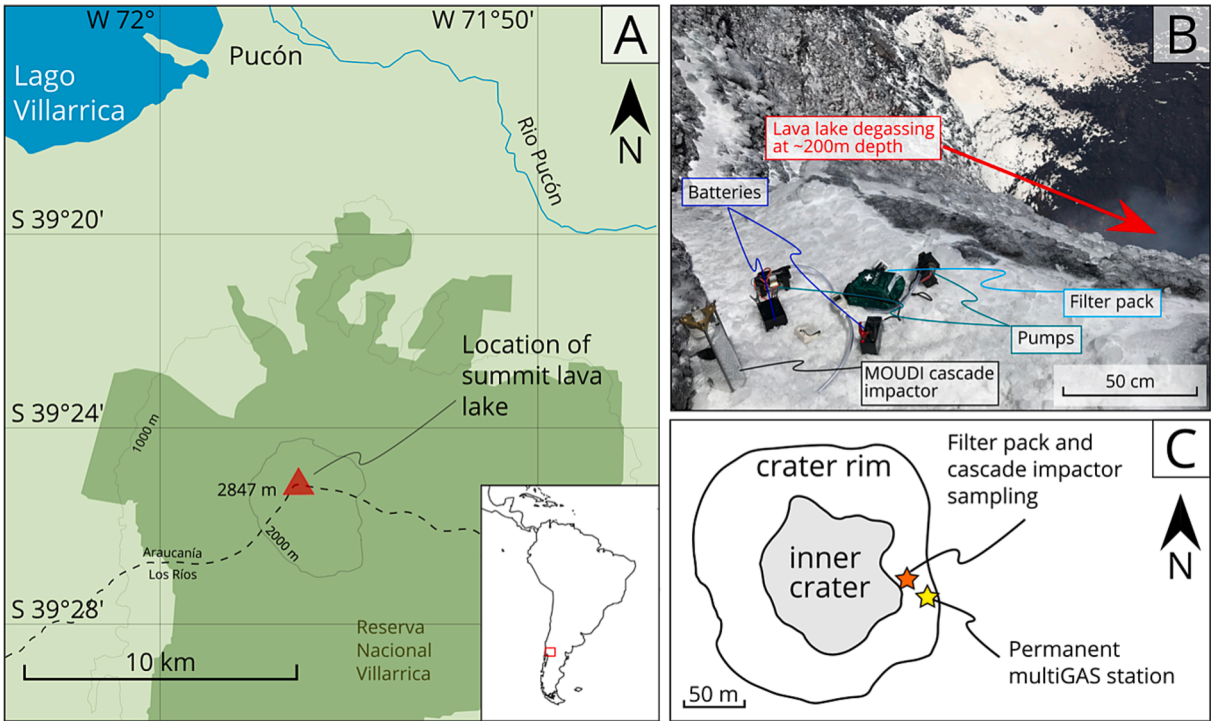

Fig. 1. Geographic location of Volcan Villarrica and sampling location. A: local map of the position of Volcan Villarrica, inset map shows Villarrica's location in South America; B: picture of sampling location on crater rim; C: the summit crater is approximately 200 m in diameter. The orange star marks the location of filter pack and cascade impactor sampling in this study. The yellow star marks the location of the permanent multiGAS station, managed by the University of Palermo (UNIPA).
Adapted from Liu et al., 2019

ppb) have been observed previously in plagioclase-hosted melt inclusions, as well as individual Cu- and S-rich fluid inclusions in some plagioclase crystals (Zajacz and Halter, 2009). Zajacz and Halter (2009) infer that the high concentrations of Cu in the melt inclusions resulted from heterogeneous entrapment at subvolcanic pressures (170–240 MPa) of silicate melt with a sulfur-rich, chlorine-poor high-temperature magmatic vapor phase in which Cu and Ag were strongly compatible. They also suggest that such a magmatic vapor phase may play a significant role in the transport of S, Cu and Ag within or between magmatic reservoirs and, consequently, in the formation of porphyry-type ore deposits. More recent studies have suggested that plagioclase-hosted melt inclusions may be enriched in Cu by post-depositional diffusive processes, whereby Cu exchanges for hydrogen during shallow degassing (Audétat et al., 2018).

In this paper we investigate chalcophile element abundance in melts and volcanic gases at Villarrica Volcano to better understand which elements are enriched in arc melts and which elements partition into aqueous saline fluids (the precursors to volcanic gases) and to what extent. We compare the chalcophile element signature of melts (as inclusions in olivine crystals) erupted from Villarrica Volcano to that of mid-ocean ridge basalts (MORB) and continental crust. We compare the concentrations of volatile chalcophile elements in volcanic gases and aerosols (collected using filter packs and cascade impactors) to those in melt inclusions to estimate volatilities for these elements, and we quantify their degassing behaviour. To interpret these observations, we model equilibrium gas-phase speciation to understand in what chemical form the metals are transported and released into the atmosphere and to assess the role of salinity in promoting fluid-melt partitioning of chalcophile elements during crustal degassing.

2. Samples and methods

2.1. Gas and aerosol sampling methods and analysis

Detailed information on the sampling and analytical methods may be found below and in the **Supplementary Material**. Volcanic activity was at a low level during the sampling period, with the top of the magma column only visible using an Unoccupied Aircraft System (Liu et al., 2019) and a diffuse plume of gas and aerosol emanating from the crater. At the summit (Fig. 1), samples of gas and particulate matter from this plume were collected onto filters via a pump from the ambient plume. Stationary ground-based filter packs and a cascade impactor were used to collect size-segregated samples of gas and particles, following well-established techniques (Allen et al., 2000; Ilyinskaya et al., 2017; Mather et al., 2012) (Fig. 1**B, C**).

Analysis of the filter packs and the size-segregated cascade impactor samples was carried out at the University of Leeds. Major and trace elements were measured in extraction solutions by ICP-MS (Thermo iCAP Qc ICP-MS) and/or ICP-OES (Thermo iCAP 7400). Details of the analysis procedure, including discussion of errors and detection limits, are given in **Supplementary Material**. All filter pack samples were analysed at the Open University by solution ICP-MS on an Agilent 8800 ICP-QQQ instrument (with a collision/reaction cell). The standard error on repeat measurements for synthetic standards was less than 5 % for all elements measured at the OU, except Sc (6 %), Sn (47 %), Ta (12 %), Ag (7 %), Hf (8 %), W (9 %) and Th (6 %). Full sample and blank concentrations can be found in the data repository (10.17863/CAM.101999**)**.

2.2. Olivine-hosted melt inclusion sample preparation and analysis

In March 2018, tephra was collected from the 2015 paroxysm eruption deposit at the crater rim, which formed a prominent recent layer of glassy pyroclasts in the summit region and upper flanks, for analysis of olivine-hosted melt inclusions. Tephra samples were crushed, sieved and hand-picked for olivine crystals, which were mounted on glass slides and ground down until melt inclusion interiors were exposed at the surface. Exposed melt inclusions were then mounted in epoxy and further polished using progressively finer silicon pastes (see **Supplementary Material**).

Major elements in matrix glass, melt inclusions and host olivines were measured using the Cameca SX100 EPMA at the Department of Earth Sciences, University of Cambridge. Acquisition parameters, calibration materials, and estimates of precision and accuracy calculated from repeated measurements of secondary standards are presented in the **Supplementary Material**. Trace elements in melt inclusions and matrix glasses were analysed by laser-ablation inductively coupled mass spectrometry at the School of Environment, Earth and Ecosystem Sciences at the Open University. A Photon Machines Analyte G2 193 nm excimer laser system coupled to an Agilent 8800 ICP-QQQ was used according to techniques described in Jenner and O'Neill (2012).

After analysis, olivine-hosted melt inclusions were corrected for post-entrapment crystallisation (PEC) using a simple olivine addition calculation (using the measured host olivine composition) for elements measured by EMPA (details provided in **Supplementary Material**). The extent of the PEC required for each melt inclusion can be found in the data repository (10.17863/CAM.101999**)**, alongside the PEC-corrected melt inclusion data. Original melt inclusion compositions, as well as the corresponding host olivine composition used to correct the melt inclusion composition for PEC, can be found in the data repository (10.17863/CAM.101999**)**.

2.3. Correcting the particulate matter compositions for silicate ash components

The particulate matter collected on the filters of both filter packs and cascade impactors is a mixture of both silicate matter, sourced from ash and fine fragmentation, and non-silicate matter sourced from gas-to-particle conversion. To quantify the volatility of elements using their abundance in particulate matter it is necessary to determine the contribution to the particulate matter made by silicate matter (ash) (as opposed to condensed salts). For the ash correction in this study, we use a compilation of whole rock lava data for Villarrica from existing literature (Turner & Langmuir, 2015); the accepted values can be found in the data repository (10.17863/CAM.101999**)**.

We consider the concentration of element A on the filter to be derived from two volcanic components, silicate ash and non-silicate aerosol:

$$[A]_{filter} = [A]_{ash} * X_{ash} + [A]_{aerosol} * (1 - X_{ash}) \quad (1)$$

where X_{ash} is the proportion of element A on the filter that is present in the ash phase. When A is a lithophile/refractory element, we assume that the concentration of this element in the aerosol phase is zero($[A]_{aerosol} = 0$), allowing the equation to be simplified to:

$$X_{ash} = [A]_{filter} / [A]_{ash} \quad (2)$$

Here we use a combination of major and trace refractory elements to calculate X_{ash}: Fe, Al, Ti, La, Ce, Pr, Nd, Sm, Eu, Gd, Tb, Dy, Ho, Er. The higher concentrations of major elements (compared to REEs) in silicate material, allow smaller ash contributions to be resolved, and are thus more sensitive to the small amounts of ash in the volcanic plume. Weighted ash fractions (WAF) can then be calculated for each element in each sample:

$$WAF = 100 * \frac{(X_{ash} * [A]_{ash})}{[A]_{filter}} \quad (3)$$

Weighted ash fractions thus obtained describe the relative proportions of an element that are found in a silicate fraction (of known composition) versus the proportions that are found in degassed (gaseous or non-silicate aerosol) phases of volcanic emissions (where other sources, i.e., background contributions, are accounted for or shown to be negligible).

2.4. Measures of chalcophile element volatility and flux

Various approaches may be taken to quantifying the volatility of elements in volcanic plumes, including emanation coefficients and enrichment factors. The *emanation coefficient*, or *volatility*, ε_X, is calculated as the percentage of the element *X* that has degassed from the silicate melt, equal to:

$$\varepsilon_X = 100 \times \left(c_i - c_f\right)^X_{melt} / c_i^X, \quad (4)$$

where c_i is the concentration of element X in the magma prior to degassing (from melt inclusion analysis) and c_f is the concentration of element *X* in the melt after degassing (Lambert et al., 1985). We calculate the amount of element X that has degassed from the melt, $\left(c_i - c_f\right)^X_{melt}$, by scaling the amount of Cl degassed (from melt inclusion and matrix glass studies) by the measured mass X/Cl ratio in the plume (where the concentration of element X has been corrected for the presence of silicate ash, see explanation of weighted ash fraction calculation).

$$\left(c_i - c_f\right)^X_{melt} = \left(\frac{[X]}{[Cl]}\right)_{plume} \times \left(c_i - c_f\right)^{Cl}_{melt} \quad (5)$$

To estimate $\left(c_i - c_f\right)^{Cl}_{melt}$ we compared compositions of olivine-hosted melt inclusions from this study (Supplementary Material) to matrix glass compositions from previous studies at Villarrica (Pioli et al., 2015; Zajacz and Halter, 2009), yielding an average of 259 ± 110 ppm Cl degassed on eruption.

Enrichment factors describe the degree to which an element is enriched in volcanic gas and non-silicate aerosol compared to its concentration in silicate material emitted from the same volcanic vent. For the concentrations of the elements in silicate material we use a compilation of whole rock lava data for Villarrica from the literature (Turner & Langmuir, 2015); the accepted values can be found in the data repository (10.17863/CAM.101999**)**. Enrichment factors are calculated as follows:

$$EF_X = \frac{\left(X_{plume}/Y_{plume}\right)}{\left(X_{silicate}/Y_{silicate}\right)} \quad (3)$$

where X_{plume} and $X_{silicate}$ are the concentrations of the element of interest, in the measured gas and aerosol emissions and silicate material, respectively. Y_{plume} and $Y_{silicate}$ are the concentrations of a reference element (typically a lithophile) in the measured emissions and silicate material, respectively. In the literature enrichment factors are calculated using a range of reference elements, discussed in the **Supplementary Material**; here we calculate enrichment factors relative to copper.

We use the mass ratio of elements compared to chlorine, $\left(\frac{[X]}{[Cl]}\right)_{plume}$, to calculate the emission rate (ER_X) of elements in the Villarrica plume, where:

$$ER_X = \left(\frac{[X]}{[Cl]}\right)_{plume} \times ER_{Cl} \quad (4)$$

where the HCl emission rate (ER_{Cl}) is calculated using an average HCl/SO_2 gas mass ratio of 0.25 compiled from existing literature (Witter et al., 2004; Sawyer et al., 2011; Shinohara and Witter, 2005) and an emission rate of SO_2 (142 ± 17 t/day) measured during the same field campaign (Liu et al., 2019). Due to the uncertainty associated with the SO_2 emission rate and the HCl/SO_2 ratio, uncertainties associated with the (ash-corrected) multi-element emission rates are large, with most being around 50 % (see the **Supplementary Material** for more detail).

2.5. Speciation modelling of gas phase chalcophile elements

The Gibbs free energy minimisation module of HSC Chemistry (version 9.9.2, Outotec Research Oy, Finland) was used to model gas speciation in Villarrica's volcanic plume. Detailed descriptions of the model are provided in previous works (Gerlach, 2004; Martin et al., 2006; Symonds et al., 1994). Model inputs are major and trace species gas concentrations (mol% or kmol), pressure (bar), temperature (°C) and the phases expected in the plume (all gas phases available in HSC chemistry for the input elements in the model are included as expected phases, except organic phases, which are unstable at high temperatures). The equilibrium temperatures and oxygen fugacities of the various gas mixtures considered in the speciation models presented here can be calculated by considering gas-phase redox couples (Aiuppa et al., 2011; Chiodini and Marini, 1998; Giggenbach, 1996; Moretti et al., 2003; Moussallam et al., 2019), which can be converted to equations for oxygen fugacity and equilibrium temperature (see **Supplementary Material** for details). To cover a range of possible magmatic temperature we modelled the gas mixture at the point of emission at between 800 and 1200 °C. See **Supplementary Material** for a full description of uncertainties in the model.

The major gaseous species inputs for the speciation modelling are given in **Supplementary Material**, which includes literature concentrations of gas species where available. The composition of the major gases within a volcanic plume sets the oxidation state of the gas mixture, which plays an important role in the speciation of major and trace gases (Martin et al., 2006; Mason et al., 2021). At Villarrica, very few measurements have been made of trace C-, S-, O-, or H-bearing gases, such as S_2, H_2, OCS, CO, and CH_4. Therefore, we have included average basaltic arc volcanic gas concentrations (Symonds et al., 1994) of these elements in the speciation model (listed in the data repository, 10.17863/CAM.101999). Without in situ measurements of these gases in Villarrica's plume, we cannot assess the uncertainty that this introduces into the speciation model outputs; therefore, we also include a version of the model in the supplement with only the values available in the literature for Villarrica. Full details can be found in the **Supplementary Material;** in summary, we find that including trace C-, S-, O-, or H-bearing gases leads to higher concentrations of sulfide and hydride complexes (particularly for Se, and to a lesser extent for Te, Pb and As). Elements that complex predominantly with Cl are largely unaffected by the introduction of the more reduced trace gases. In order to be able to directly relate the literature major gas species compositions to those measured in our study, we use our element to Cl ratios (X/Cl) to scale the concentrations to the HCl value used in the model input compositions (please refer to the data repository 10.17863/CAM.101999**)**.

3. Results

3.1. Olivine-hosted melt inclusion compositions

The melt inclusions analysed from the 2015 eruption of Villarrica are basaltic to basaltic-andesite in composition and have experienced up to ~10 % PEC (**Supplementary Material;** Fig. 2). Major element and volatile concentrations (corrected for PEC) are shown in Figs. 2 and 3. The concentrations of PEC-corrected volatiles sulfur (S) and chlorine (Cl) and K_2O in the melt inclusions are shown in Fig. 3. Major element variation are consistent with crystallisation trends (decreasing Al_2O_3, CaO and increasing K_2O with SiO_2 concentrations). The highest volatile (S, Cl) concentrations occur in the most primitive glasses, suggesting that degassing accompanied crystallisation, as observed elsewhere (Blundy and Cashman, 2005).

Trace element (including chalcophile element) compositions of the melt inclusions are shown in Fig. 4 normalised to parental MORB (Fig. 4**a**) and average continental crust (Rudnick and Gao, 2003) compositions (Fig. 4**b**) and plotted in order of bulk compatibility with respect to a typical MORB assemblage (Jenner, 2017). Also shown are whole rock data from Antuco Volcano, Chile (Cox et al., 2019). Villarrica melt inclusions show substantial enrichments in Sb (100–120 x), Pb (95–110 times), Tl (30–80 times), W (80 to 120 times) and U (30–70

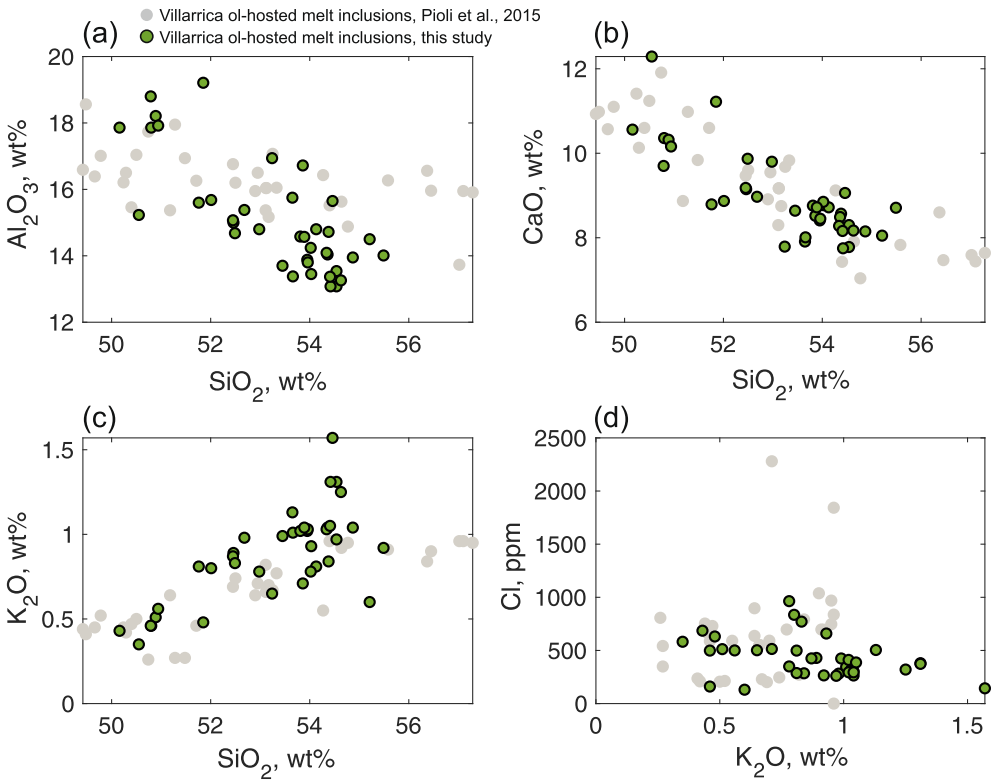

Fig. 2. Major and volatile element concentrations in olivine-hosted melt inclusions in erupted products from the 2015 paroxysm at Villarrica Volcano, Chile, measured using electron probe micro-analysis (green). Also shown are olivine-hosted melt inclusions associated with the products of the Chaimilla eruption of Villarrica Volcano, ~3100 yr BP (Pioli et al., 2015).

times) and a weak enrichment in Cu (2–3 times) relative to MORB; and moderate enrichments in Cu (9–10 times) and weak enrichments in Cs (up to 2 times), Sb (2–3 times) relative to the average composition of continental crust (Rudnick and Gao, 2003) (Fig. 4).

3.2. Volcanic gas and particulate compositions

Concentrations of trace and major elements measured in Villarrica's volcanic gas and aerosol plume are in the data repository (10.17863/CAM.101999) and range in magnitude from 10^{1} μg m^{-3} for major refractory elements (e.g., Fe, Ca) to 10^{-6} μg m^{-3} for some rare earth elements before an ash correction is performed.

Weighted ash fractions (WAFs) for the range of elements measured in the filter samples are shown in Fig. 5, with elements coloured according to their geochemical affinity (chalcophile, lithophile etc). The analysis shows that many of the lithophile elements measured on the filters were largely delivered via a silicate particulate phase. Major elements such as Al, Ca, Fe and the REE have WAFs of 100 %, indicating they exist in the volcanic plume predominantly in the silicate phases. In contrast, the chalcophile elements, large ion lithophiles and volatiles S and Cl have low WAFs: Tl, S and Cl have WAFs > 0.01, suggesting they are partitioned overwhelmingly into the gas phase. Chalcophile elements such as Sb, Pb, Sn, Cu, Mo and Pb have WAF values ranging from 0.2 to 1 % (Fig. 5).

Size-segregated particulate matter data collected using the cascade impactor may be found in the data repository (10.17863/CAM.101999) and Fig. 6. The two samples were collected on different days, with sample M1 collected over ~3 h, and sample M2 collected over ~4 h 20 min. In sample M1, collected on 15/03/18, size-segregated concentrations of elements were shifted to coarser size bins than for sample M2, collected on 25/03/18 (Fig. 6). Highly volatile metalloids such as Se and As were not detected in M1 but were detected in M2. In M2, several refractory elements (e.g., Er, Co) were only detected in one size bin, whereas in M1, they were detected in several size bins. Further, in M2 several refractory elements (e.g., Ho, Yb, Mo) were below detection limits in all size bins (detection limits in the data repository, 10.17863/CAM.101999) but were detectable in at least one size bin in M1.

Filter pack samples collected on the same day as the M1 cascade impactor sample typically have higher calculated silicate ash fraction (WAFs) than those collected on the same day as M2, especially for volatile elements such as K, Cu, Zn, Sn, Pb, Cl and S. Greater ash contributions to the impactor sample on 15/03/2018 are also supported by the presence of certain refractory elements above detection limit in M1 but not in M2 (e.g., Ho, Yb) despite the fact that sample M2 was sampling the plume for over an hour longer than M1 (detection limits in the data repository, 10.17863/CAM.101999).

Gases typically cool, oxidise and quench as they mix with the ambient atmosphere, then condense to form particulates after emission from a high temperature source, with sizes at the upper end of the nucleation mode ($D < 0.1$ μm); thereafter particles may grow by further condensation or agglomeration to reach sizes consistent with the accumulation mode (0.1 μm $< D <$ 2 μm). The 'coarse particle' mode ($D > 2$ μm) is composed largely of mechanically generated particles, e.g., ash (Whitby, 1978). Volatile trace elements are typically found most abundantly in the 'accumulation' and coarse modes, from 0.18 to 1.8 μm (Fig. 6), consistent with other size-segregated particulate measurements made at Kīlauea Volcano, Hawai'i (Mason et al., 2021; Mather et al., 2012). The size-distributions of volatile S and Cl differ between the two sampling days: on 15/03/2018 (sample M1) both S and Cl are collected with diameters typically associated with the accumulation mode, while on 25/03/2018 (sample M2) Cl was found mainly in the nucleation mode, and S found mainly in the coarse particle mode.

In contrast to the more volatile elements, concentrations of refractory elements such as Ca, Mn, Na, and many of the REEs are distributed evenly across size bins within the nucleation, accumulation and coarse particle modes. Given that this pattern is repeated across

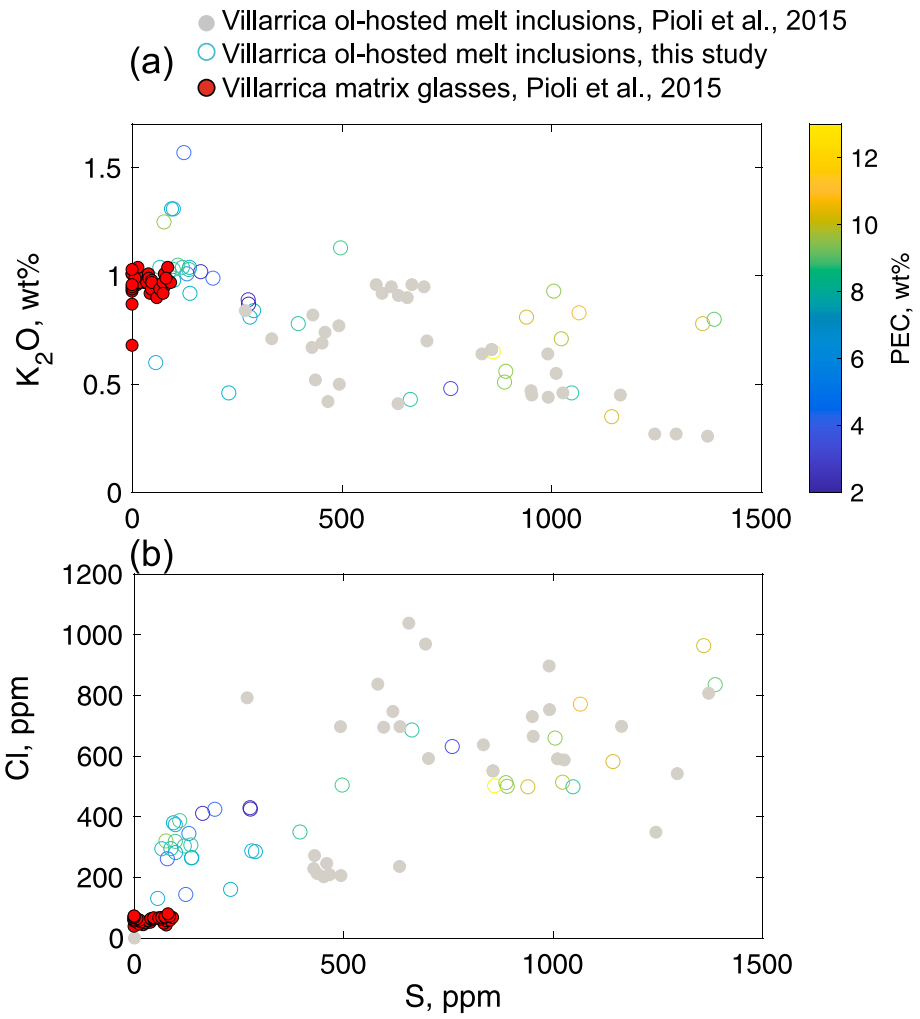

Fig. 3. A comparison of matrix glass (MG) and melt inclusion (MI) compositions (S and Cl) for Villarrica. Data presented in this Figure includes MI data from this study (coloured for the extent of post-entrapment crystallisation, see key), and from the older Holocene 3100 yr basaltic-andesite erupted products from Villarrica (in grey) (Pioli et al., 2015; Zajacz and Halter, 2009). Matrix glass compositions from Pioli et al., (2015) are shown as red filled circles.

many refractory elements, we can infer a similar source for these elements, which is most likely to represent fine ash with a range of diameters. There are some refractory elements that appear to be exceptions to this rule (e.g., Ba, Co, Ho, Yb) however, it is likely in these cases that the measured concentrations of these elements were insufficient to be above detection limits on all the stages of the cascade impactor.

In Fig. 6 we show the calculated solubility of each element in water. Solubility in water was calculated from the mass of the element extracted from the filters in water at room temperature and compared with the mass of the element extracted in the later acid stage (see **Supplementary Material** for details). Solubility values are significantly different between volatile (mostly >50 %) and refractory (mostly <50 %) elements, consistent with the low solubility of silicate material (Ilyinskaya et al., 2021; Mather et al., 2012), which is the source of most of the refractory elements. Volatile elements are carried as water-soluble particles at Villarrica (e.g. as chlorides, sulfates, oxides) as has also been shown to be the case at Kīlauea Volcano, Hawai'i (Ilyinskaya et al., 2021; Mather et al., 2012).

We calculate enrichment factors (EFs) relative to Cu for the ash-corrected filter pack data for those elements for which silicate compositions are available, shown in Fig. 7. We see that chalcophile trace elements are highly enriched in the volcanic gas plume relative to silicate melt, testifying to their volatile nature. In particular, Sb, Sn, Cu, Mo, Pb and Tl show strong volatile tendencies, with EFs 50–100 times larger than the lithophile REE (Fig. 7) and Tl exhibiting an enrichment factor similar to chlorine (Cl). The EFs calculated for Villarrica are compared to EFs (calculated relative to Cu) for Etna (Aiuppa et al., 2003) and Stromboli (Allard et al., 2000). The trends in all datasets are broadly similar, albeit with more scatter in the Etna dataset (Fig. 7). The slightly higher EFs on average for the full range of lithophile elements may be accounted for by different methods to calculate WAFs.

We compare the element-to-chlorine (X/Cl) ratios of elements in high temperature volcanic gas and aerosol plume emissions for a set of basaltic to basaltic-andesite arc and intraplate volcanoes (Fig. 8**a**). Mass X/Cl in the gas and aerosol phase typically varies by two orders of magnitude or more between volcanoes for many elements such as Cu, Pb, As, Tl, W, Cs.

Fluxes of volatile chalcophile elements emitted from Villarrica in the gas and aerosol phase during March 2018 are shown in Fig. 8**b** and the data repository (10.17863/CAM.101999). Fluxes of As and Cu ranged from 10 to 80 kg/day, and fluxes of Pb, Cd, Zn and Tl from 1 to 7 kg/day (Fig. 8**b**). These fluxes are 1–2 orders of magnitude lower than those calculated for Stromboli and Etna (300–10,000 kg/day Cu), for example, but similar to those measured during the large basaltic fissure eruptions of Kīlauea in 2018 (Mason et al., 2021) and Holuhraun in 2015 (Gauthier et al., 2016).

We calculate emanation coefficients (ε) for elements where corresponding silicate compositions are available (the data repository, 10.17863/CAM.101999). Average emanation coefficients for each element

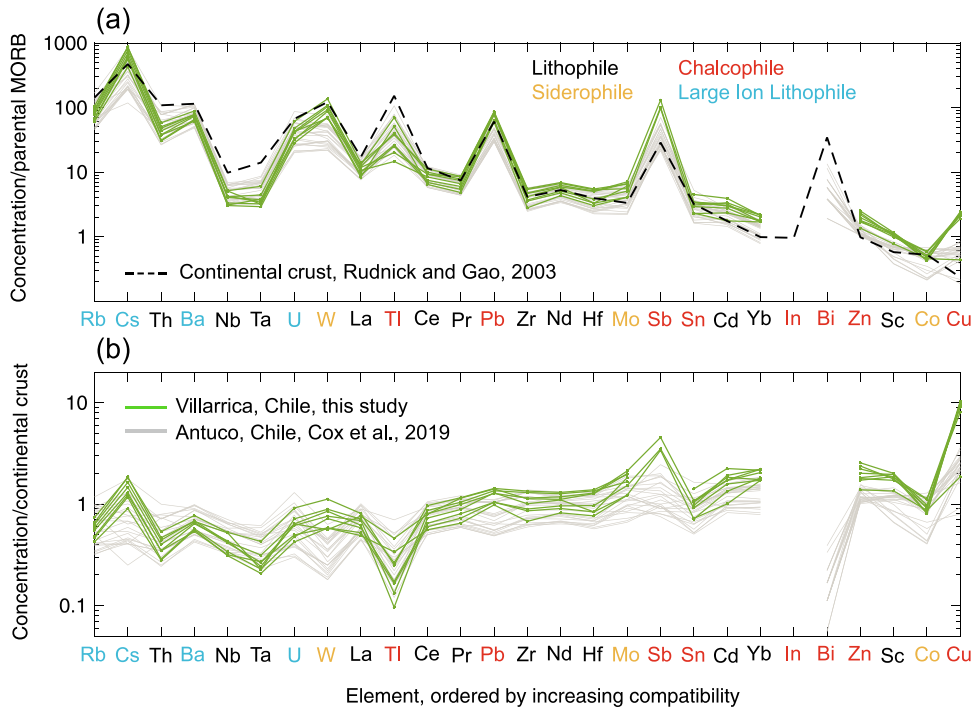

Fig. 4. Trace element composition of olivine-hosted melt inclusions from Villarrica, Chile (in green) measured by laser ablation ICP-MS. (a) Trace element concentrations normalised by parental MORB compositions (Jenner, 2017). The composition of continental crust (Rudnick and Gao, 2003) is also shown. Whole rock compositions for Antuco Volcano are also shown (Cox et al., 2019). (b) Trace element concentrations normalised by continental crust composition.

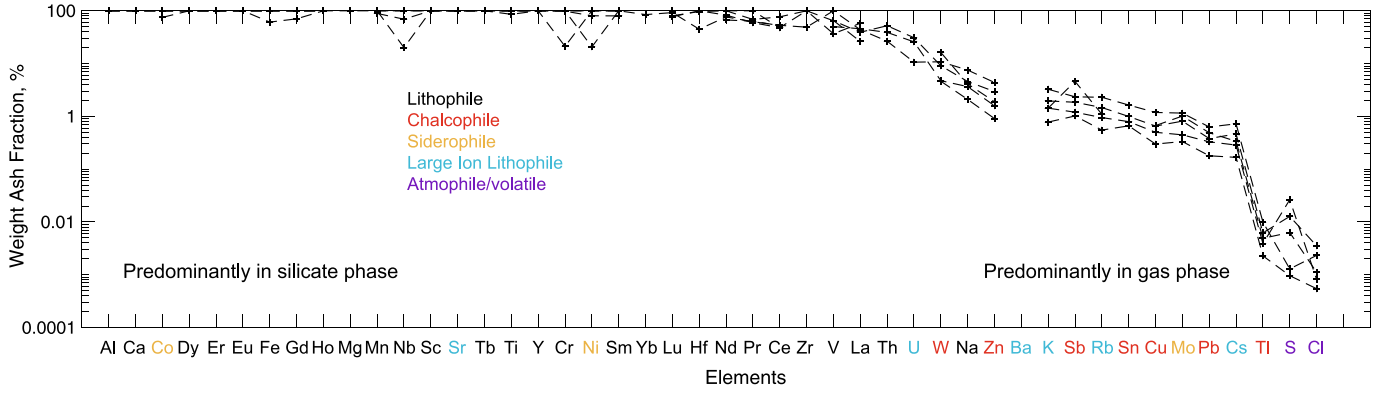

Fig. 5. Weighted ash fractions (%) calculated for all filter pack samples. Saturated filter pack sample V2 L3 can be included here as the WAF calculation does not rely on gas compositions. The ash correction method used to calculate WAFs can be found in **Supplementary Material**. Full WAF data and associated propagated errors are given in the data repository (10.17863/CAM.101999).

are shown plotted against mass HCl/SO_2 (measured variously using spectroscopy and direct sampling; data citations in the caption) in the gas phase in Fig. 9**,** along with data from other intraplate (pink shading) and arc (blue shading) volcanoes, to assess how the volatility of each element varies with gas chloride content. Enrichment factors calculated for Villarrica are consistent with those calculated for other basalt to basaltic andesite volcanoes and in general range up to a few % for moderately volatile elements such as Pb, Cd, Zn, Bi, As, Sb and a few tens of % or more (some approach 100 %) for the most volatile elements Tl, Se, Te, Re (Fig. 9). Emanation coefficients for elements that show a strong affinity for chloride during degassing (e.g., Zn, Cu, Ag and Cs) are positively-correlated with increasing HCl/SO_2 gas ratios for the datasets shown in Fig. 9, with emanation coefficients at arc volcanoes typically 1–3 orders of magnitude higher than those at intraplate volcanoes, with little overlap.

3.3. *Chalcophile element speciation in volcanic gases*

We modelled the equilibrium speciation of metal and metalloid elements in Villarrica's volcanic plume at the point of emission at the lava-air interface (Figs. 10, 11). We provide a comparison speciation model for Kīlauea Volcano, Hawaii (Mason et al., 2021). Using different combinations of redox couples (**Table S3, Supplementary Material**), we calculate average oxygen fugacities (log fO_2) of −9.6 and −11.4 for Villarrica and Kīlauea gas mixtures, respectively. Since the oxidation state of volcanic gases is strongly temperature-dependent, we have compared the two plume compositions at the same temperature (1150 °C) (Fig. 11). Volcanic gases at Villarrica have higher chlorine and water contents than Kīlauea (Villarrica: 0.8 mol% HCl, 93 mol% H_2O; Kīlauea: 0.2 mol% HCl, 80 mol% H_2O; **Table S3, Supplementary Material**). As a result, there are some notable differences between the speciation of metal and metalloid elements between these two basaltic volcanoes

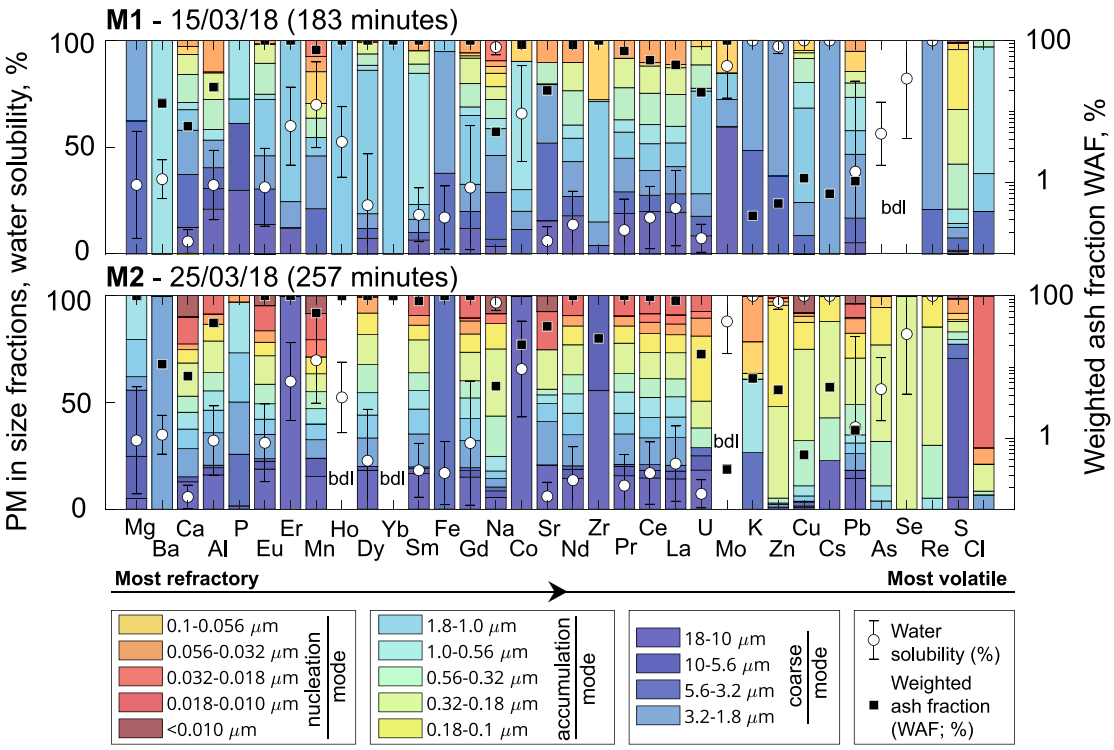

Fig. 6. Size-segregated concentrations of elements in the Villarrica plume for two cascade impactor samples: M1 and M2 (sample acquisition timescale is shown in brackets). Elements are shown in order of increasing volatility (from this study) from left to right. Sc, Lu, Ta, V, Sn, Sb are below detection limits (bdl) on all collection stages. Solubility in water (white circles) is calculated as the proportion of an element that is measured in the water extraction versus the acid extraction, as outlined in the **Supplementary Material**. Weighted ash fractions are black squares. A discussion of propagated errors can be found in the data repository (10.17863/CAM.101999).

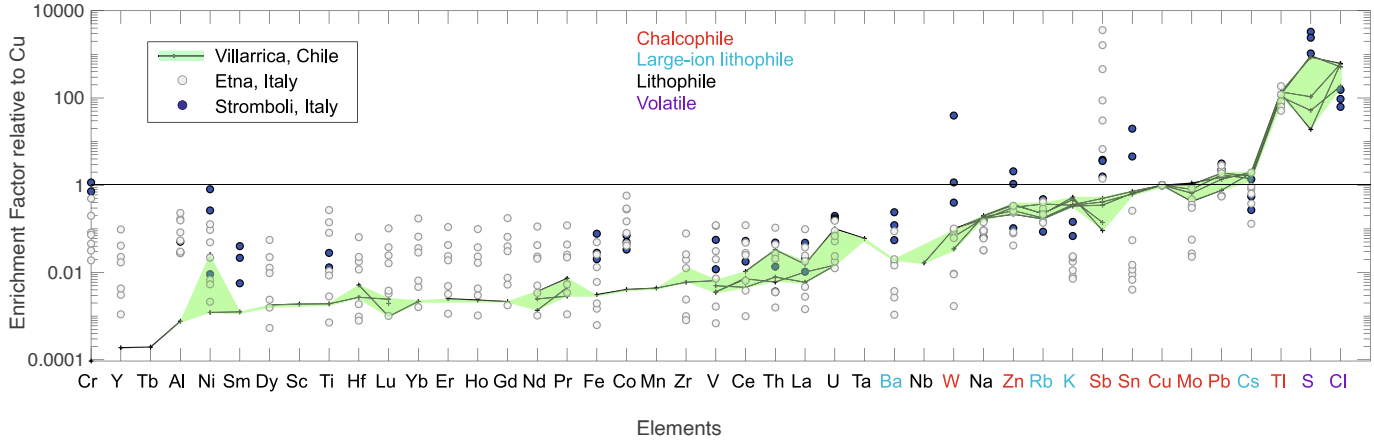

Fig. 7. Volcanic gas and aerosol plume composition shown in terms of enrichment factors referenced to Cu, defined by $[X/Cu]_{gas}/[X/Cu]_{silicate\ melt}$ calculated using filter pack data and ordered by the EF for the Villarrica data. Data for Etna (Aiuppa et al., 2003) and Stromboli are also shown (Allard et al., 2000). Data can be found in the data repository (10.17863/CAM.101999).

(Figs. 10, 11). For Kīlauea, Te, Se, Pb, and As are predominantly (>75 mol%) complexed as sulfide gas species, while at Villarrica, sulfide complexes make only a minor (<20 mol%) contribution to the equilibrium speciation of these elements (Fig. 10). We attribute these differences to the greater availability of S at Kīlauea (e.g., 13.6 mol% for Kīlauea versus 1.8 mol% SO_2 for Villarrica) and the higher oxygen fugacity of the gas mixture at Villarrica (**Table S3**, **Supplementary Material**), which acts to suppress the availability of reduced sulfur. **Fig. S2** (**Supplementary Material**) compares the dominant speciation of sulfur in Villarrica and Kīlauea's plumes over a range of magmatic temperatures (800–1200 °C). For both plumes, the majority of sulfur is present as SO_2 (S oxidation number = +4) gas across the range of temperatures; however, for Villarrica, concentrations of S_2 (di-sulfur; S oxidation number = 0) gas are at least an order of magnitude lower than those at Kilauea. Concentrations of H_2S (S oxidation number = −2), SO (S oxidation number = −2) and S_2O (S oxidation number = −1) are also higher for the Kīlauea volcanic gas mixture.

A greater proportion of some elements (e.g., Zn, Pb, Cu and Ag) are present as chloride gaseous species in Villarrica compared to Kīlauea (Figs. 10, 11). Villarrica's gas emissions are rich in chloride ligands compared to Kīlauea's, and previous work has shown that more oxidised gas mixtures (such as Villarrica's volcanic plume) lead to higher

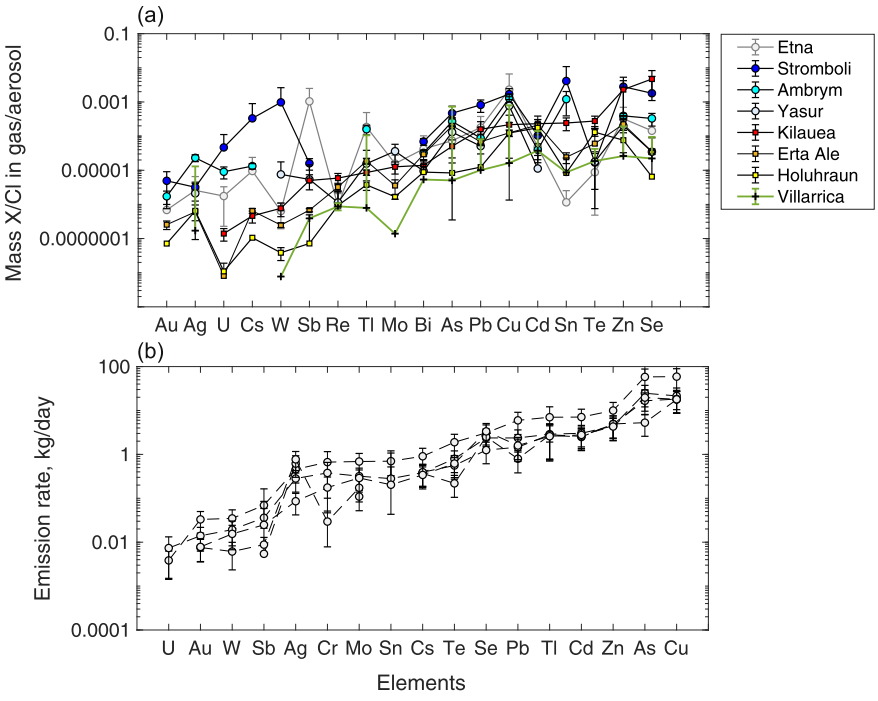

Fig. 8. Volcanic gas/aerosol mass X/Cl ratios and emission rates of trace metals via the gas and aerosol phase as measured in the Villarrica gas plume in March 2018. (a) X/Cl mass ratios in emissions from basaltic to basaltic-andesite volcanoes at different tectonic settings. Data sources are as follows: Holuhraun 2015 (Gauthier et al., 2016); Kīlauea 2008 (Mather et al., 2012); Kīlauea 2018 (Mason et al., 2021); Erta 'Ale 2011 (Zelenski et al., 2013); Etna 2001 (Aiuppa et al., 2003); Ambrym 2007 (Allard et al., 2016); Stromboli 1993–97 (Allard et al., 2000); Yasur 2016 (Mandon et al., 2019); Villarrica 2018 (this study); (b) Emission rates of various elements from Villarrica via the gas and aerosol plume, in kg/day. Vertical bars are the uncertainty on the fluxes (data repository (10.17863/CAM.101999) and error propagation is discussed in Supplementary Material).

concentrations of reactive halide species, thus increasing the availability of chloride ligands (Gerlach, 2004; Martin et al., 2006).

At the high temperatures of magmatic degassing (800–1200 °C), Cu exists mainly as chloride complexes. At Kīlauea, where the chloride content of the volcanic gases is relatively low (Fig. 9), ~70 % of Cu is found in chloride gaseous species at equilibrium (versus close to 100 % for Villarrica; Fig. 11). It has been shown that reducing the chloride content of Kilauea's gas further, down to 1 % of the actual chloride concentration of Kīlauea's volcanic plume, speciation models predict that only one third of the Cu in the speciation model will exist as chloride complexes (Mason et al., 2021). Zn shows some affinity for Cl at equilibrium in Villarrica's plume, but is predominantly present as a free gas ($Zn_{(g)}$). Fig. 9 shows that both Zn and Cu emanation coefficients increase with increasing HCl/SO_2 gas ratios, by up to 4 and 5 orders of magnitude respectively. Ag also shows strong affinity for chloride in equilibrium speciation models, but like Zn, it also degassed as a free elemental gas ($Ag_{(g)}$). However, Ag's affinity for Cl is stronger than Zn, with ~50 % of Ag degassing within chloride complexes at Villarrica, versus ~15 % of Zn. This higher affinity for chloride, combined with enrichments of Ag in arc melts, may explain why Ag is enriched in arc emissions to a greater extent than Zn (Fig. 9).

Emanation coefficients for Cs, Ag, and Tl also increase with increasing HCl/SO_2 ratios, although across a narrower range of values than for Cu and Zn (over approximately 3 orders of magnitude versus 4–5 for Zn and Cu). Similar to Cu, Cs shows strong affinity for chloride (Fig. 10) in equilibrium speciation models for both Kīlauea and Villarrica (Figs. 10, 11); this may suggest that when Cl availability in the vapour phase is lower, degassing of Cs from the silicate melt into the vapour phase will be suppressed (i.e., its emanation coefficient will be lower).

Speciation models suggest that Tl shows little affinity for S- or Cl-bearing ligands and is present predominantly as an oxide species in both Kīlauea and Villarrica equilibrium speciation models (black dashed outline in Fig. 10). The second most abundant Tl-bearing gas is $TlCl_{(g)}$, but at several orders of magnitude lower concentrations than $TlO_{(g)}$. $TlCl_{(g)}$ concentrations are predicted to be slightly higher in the Villarrica's plume but are still very low. Therefore, speciation models cannot explain the positive correlation between emanation coefficients for Tl and HCl/SO_2 ratios (Fig. 9) as it can for Cs, Ag and Cu. Zelenski et al., (2021) showed that Tl partitions into the fluid phase more strongly at arcs (HCl-rich) than at hotspot/rift volcanoes (S-rich). Since there are predicted differences in the speciation of Tl between Villarrica and Kīlauea, the higher emanation coefficient for Tl in volcanic arcs may be linked to other factors, such as the availability of water or the higher oxygen fugacity of arcs (**Table S3, Supplementary Material**).

Elements that show very little affinity for Cl^- and/or a strong affinity for S^{2-} (e.g., Te, As, Se) (Figs. 10, 11), or that show little affinity for either ligand (e.g., Re, Cd) (Figs. 10, 11), do not display strong correlations between ε values and HCl/SO_2 ratios, and ε values overlap considerably between arc and intraplate volcanoes (Fig. 9) (Zelenski et al., 2021). However, Re and Cd concentrations in arc melts are poorly constrained and further data are needed to better assess the volatility of these elements.

Lead displays a strong affinity for both S (<90 % of Pb is complexed with S^{2-} in the Kīlauea equilibrium speciation model) and Cl (~60 % of Pb is complexed with Cl^- in the Villarrica equilibrium speciation model). With this 'flexible' speciation, we might expect that Pb degassing is relatively unaffected by changes in the proportions of S and Cl ligands, i.e., the extent to which it degasses from the melt into the fluid phase is similar between arc and intraplate volcanoes. This is supported by partition coefficients calculated by Zelenski et al., (2021), which indicate that there is a relatively small difference in Pb silicate melt-fluid partitioning between more Cl-rich arc settings and more S-rich hotspot/rift settings. We also find in this study that Pb emanation

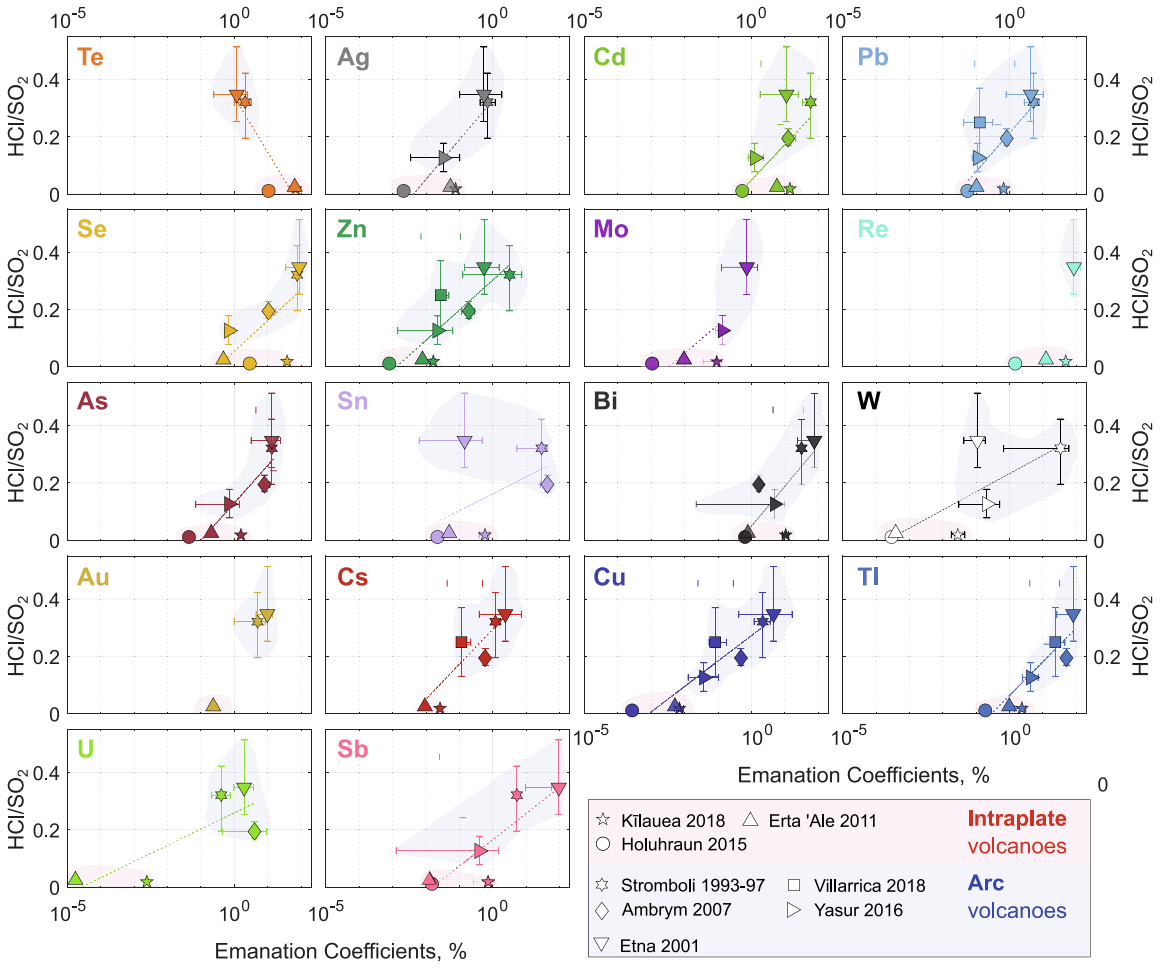

Fig. 9. Emanation coefficients (ε) versus HCl/SO_2 gas phase mass ratios. Volcanic gas data are from this study (Villarrica) and from the literature (Aiuppa et al., 2003; Allard et al., 2000; Allard et al., 2016; Gauthier et al., 2016; Mandon et al., 2019; Mason et al., 2021; Zelenski et al., 2013).

coefficient values for basaltic intraplate volcanoes are comparable to those for some arc volcanoes (Fig. 9) despite differences in HCl/SO_2 gas ratios. Despite the comparable partitioning/emanation coefficient values Pb is enriched in arc volcanic gas emissions compared to intraplate emissions (Zelenski et al., 2021), which can be mainly attributed to the greater enrichment of Pb in arc silicate melts due to slab devolatilisation (Fig. 4).

Other elements that show a strong affinity for S^{2-} during degassing (at Kīlauea) are As, Se and Te; more than 70 % of the concentrations of these elements in Kīlauea's plume degas as sulfide species at 1150 °C and atmospheric pressure. Lower S^{2-} availability at Villarrica (**Fig. S4, Supplementary Material**) means that Se and Te degas as a mixture of hydride, sulfide and free gas species, while As degasses predominantly as an oxide gas species (Figs. 10, 11). The volatility of Se and Te at subaerial arc volcanoes are comparable to (Se) or lower (Te) than that for intraplate volcanic systems (Fig. 9). Partition coefficients for As, Se and Te calculated by Zelenski et al., (2021) indicate that fluid-melt partitioning is more extensive at S-rich intraplate subaerial volcanoes compared to Cl-rich arc subaerial volcanoes, with this difference in partitioning largest for Te, which is in agreement with the higher emanation coefficients for Te in intraplate settings presented in Fig. 9.

4. Discussion

4.1. Enrichments of fluid-mobile elements in Villarrica magma

Villarrica basaltic andesite melts show enrichments in the large ion lithophile elements (including Cs) and in the chalcophile elements W, Tl, Pb and Sb over MORB (Fig. 4). Previous studies of both back-arc basin glasses (Jenner, 2017) and arc whole rocks (Cox et al., 2019; Noll Jr et al., 1996) have shown similar enrichments in these elements over MORB, with the addition of Bi and As (Jenner, 2017) (Fig. 12). Jenner (2017) speculated that As–Tl–Pb–Sb–Bi may be delivered to the mantle wedge via fluids produced during the breakdown of host-phases in the upper oceanic crust during subduction, e.g. hydrothermal sulfides and serpentinites. It has been shown that Tl is highly enriched in metalliferous sediments that enter subduction zones, due to adsorption onto authigenic Fe–Mn oxy-hydroxides (Shaw, 1952); this has led to the use of Tl isotopes as a sensitive tracer for pelagic sediment input to arcs (Nielsen et al., 2017). Studies of oceanic serpentinites in the Atlantic show they are highly enriched in aqueous fluid-mobile elements including As, Sb, Cs, Pb, and this has been suggested as a principal mechanism for transporting fluid mobile elements into subduction zones (Deschamps et al., 2011). Transformation of antigorite to olivine at high pressures in the subducting slab results in the release of fluids with high concentrations of Cl, Cs, Pb, As, Sb, Ba, Rb, B, Sr, Li and U, up to several orders of magnitude higher than that of primitive mantle, bearing a similarity to the enrichments observed in arc magmas (Wu et al., 2020). A recent study suggests that breakdown of sulfides hosted by oceanic basalts on the down-going slab may supply the bulk of the Cu, As, Ag, Cd and Te in slab fluids (Walters et al., 2021). Other studies have proposed that melts produced from sediments on the down-going slab are an important source of chalcophile elements to the melting regions beneath arcs (D'Souza and Canil, 2018). Experiments at 1000 C and 3 GPa on

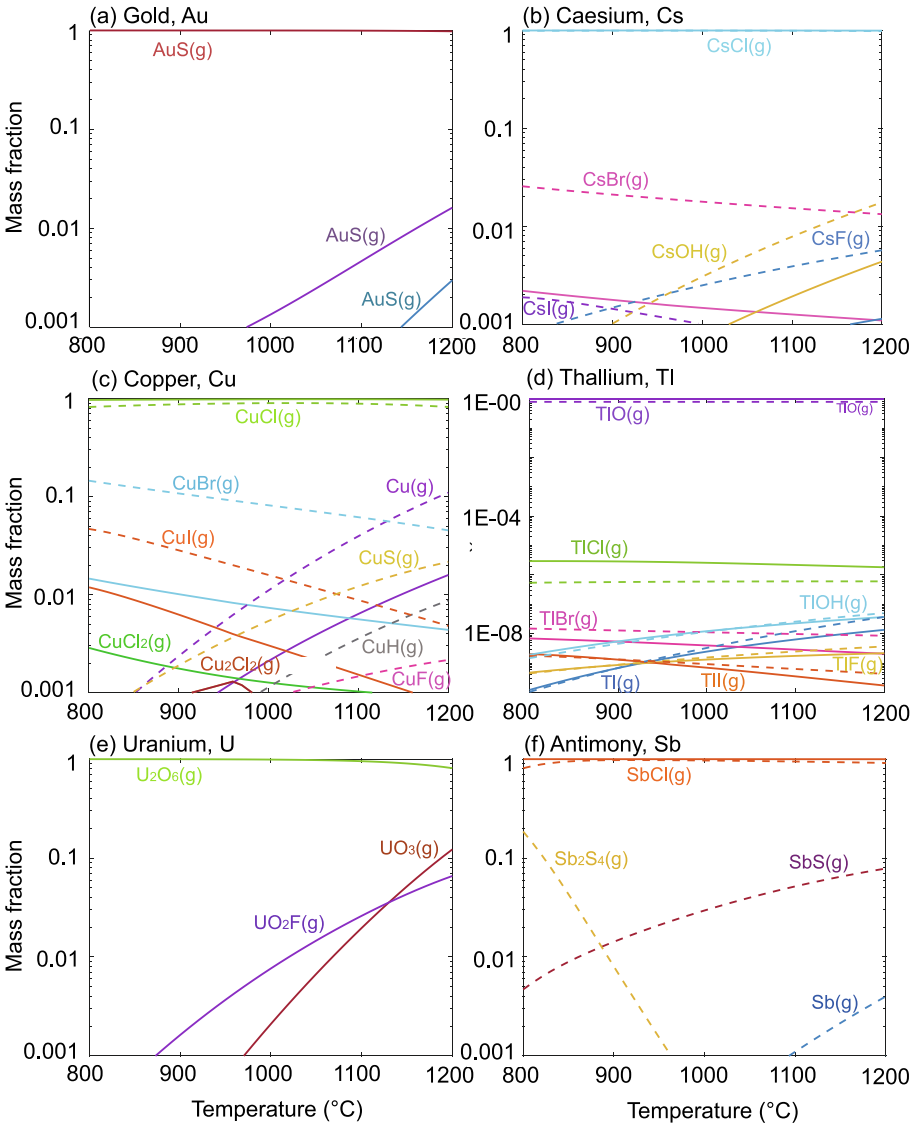

Fig. 10. Major gaseous species in equilibrium speciation model outputs for Villarrica (solid line) and Kīlauea's (dashed line) volcanic gas plumes. Mass fractions are the mixing ratios of the concentration of the gas in question over the total concentration of all gases bearing that element in the mixture. Equilibrium speciation model input and output data can be found in the data repository (10.17863/CAM.101999).

fluid-saturated pelite melts to determine fluid-melt partition coefficients of chalcophile elements show that Mo, Pb, As, and Sb are highly fluid-mobile under reducing conditions (where sulfide, rather than sulfate is stable) and much less fluid-mobile under oxidised, sulfate-present conditions (D'Souza and Canil, 2018).

4.2. Degassing of Villarrica magmas

The chalcophile-enriched basalts generated in the mantle wedge undergo differentiation (concurrent fractionation, degassing and mixing) in crustal magma storage regions beneath Villarrica Volcano, likely over a range of depths. Volatiles released during crystallisation and ascent (decompression) supply a persistent gas plume to the atmosphere, likely generated by sustained magma supply and second boiling, as well as shallow magma convection within a conduit (Edmonds et al., 2022; Liu et al., 2019; Moussallam et al., 2016). The lack of Cu depletion in the Villarrica melt inclusions relative to MORB and continental crust (Fig. 4) suggests the basalts have not undergone significant sulfide fractionation prior to melt inclusion entrapment, although we cannot rule out diffusive modification of the melt inclusions (Audétat et al., 2018). Similarly, unlike other Chilean arc magmas which show a decrease in Cu and Cu/Ag with decreasing MgO, which may be attributable to monosulfide solid solution fractionation (Cox et al., 2019), Villarrica whole rock analyses show an increase in Cu and constant Cu/Ag, which indicates that the Villarrica magmas remained sulfide-undersaturated until at least ~4 wt% MgO during differentiation (Cox et al., 2019). Previous studies have found no magmatic sulfide inclusions in Villarrica rocks (Grondahl and Zajacz, 2022; Zajacz and Halter, 2009).

The chalcophile elements and the large ion lithophile Cs are strongly enriched in the volcanic gas and aerosol phase relative to silicate melt at Villarrica (Fig. 7). This enrichment is up to 6 orders of magnitude greater than the lithophile REE for some elements (Tl) and 3 orders of magnitude greater than the lithophile REE for most of the other chalcophiles (Cu, W, Zn, As; Fig. 7). The enrichment of these elements in the gas phase suggests that these elements partition into an aqueous saline exsolved volatile phase during magma storage in the crust and then, at low pressures, form part of low-density volcanic gases that condense upon emission into the atmosphere into fine particulate water-soluble aerosol (Fig. 6). Emanation coefficients (or volatilities) are between 12 and 45 % for Tl, with most other chalcophile elements such as Pb, Sn and Mo displaying volatilities of up to 0.3 % and 0.05–0.08 % for Cu (**data repository** 10.17863/CAM.101999). The volatilities of Re, Te and Se, as

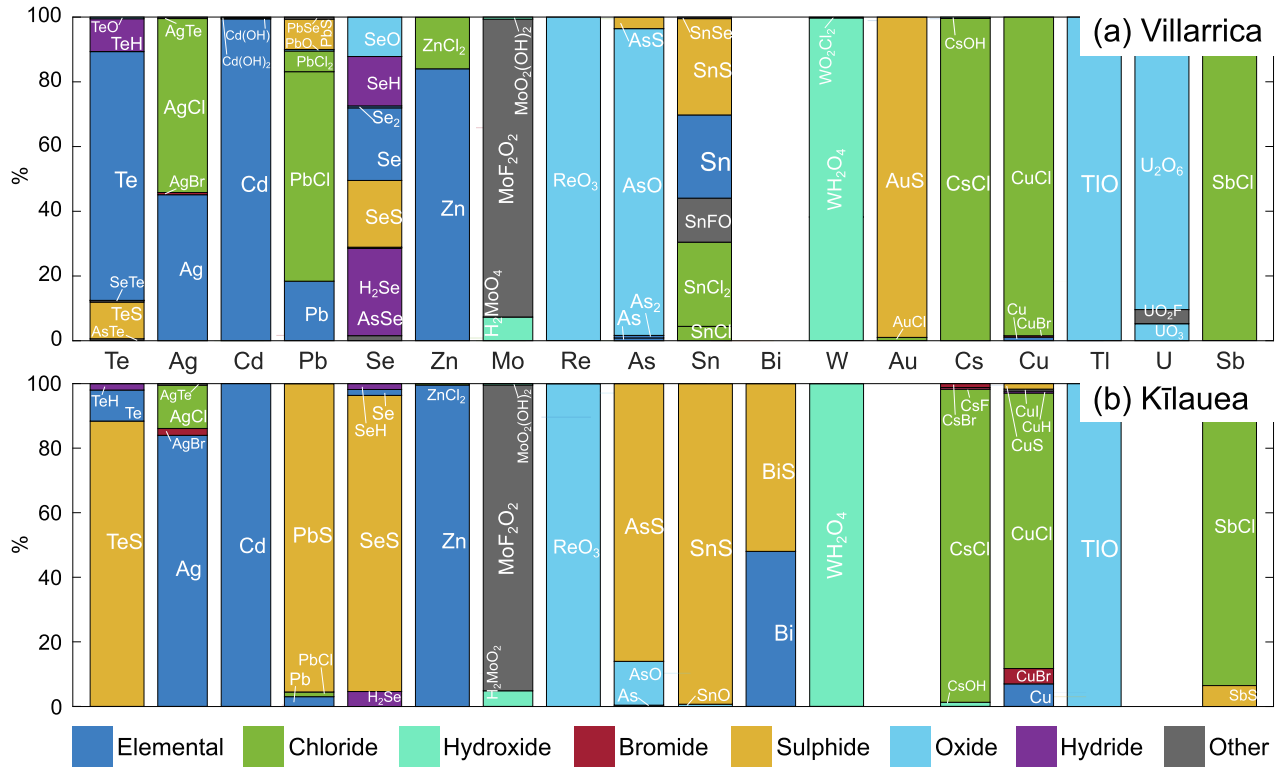

Fig. 11. Equilibrium speciation model outputs for volcanic gases at 1150 °C for Villarrica and Kīlauea volcanoes. Speciation is presented here in broad ligand groupings. For the specific species that make up the results of both models, and how they differ between the two volcanoes, see **Supplementary Material S5**. Equilibrium speciation model input and output data may be found in the data repository (10.17863/CAM.101999).

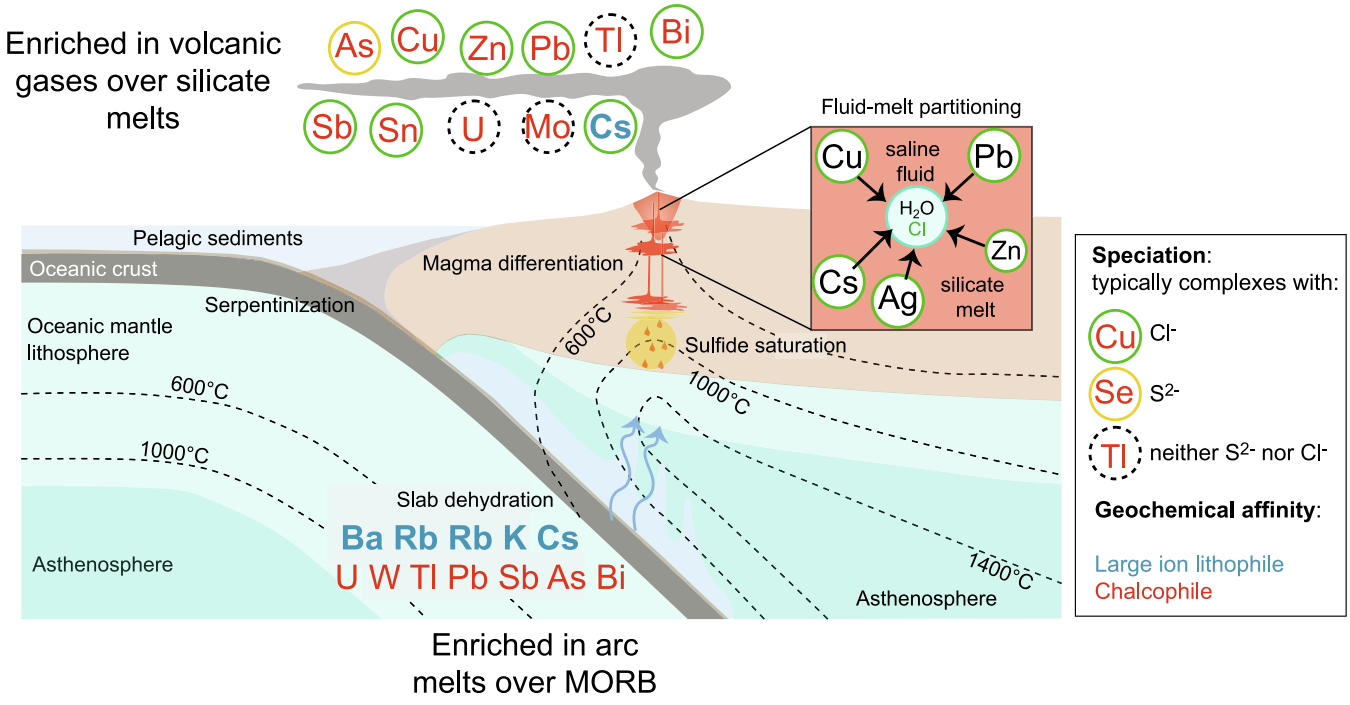

Fig. 12. Summary diagram to show lithophile and chalcophile processing through a schematic subduction zone. Lithophile and chalcophile elements are transferred from the downgoing slab to the overlying wedge via fluids generated from the dehydration of sediments, hydrothermal sulfides and serpentinised oceanic lithosphere, thereby enriching arc melts in these elements over mid-ocean ridge basalts (this work; Cox et al., 2019; Jenner, 2017). Villarrica melts have not undergone sulfide saturation and sequestration in the crust, and therefore have no Cu depletion. Primitive melts have undergone differentiation, which may involve crystallisation, mixing and degassing, during storage in the continental crust. Chalcophile elements and Cs partition into a saline exsolved magmatic fluid phase. Volcanic gases are the low-pressure manifestation of this exsolved volatile phase. Chalcophile elements and Cs are enriched by up to 6 orders of magnitude in the volcanic gas over the silicate melt, relative to involatile elements (e.g. REE). Many of the chalcophile elements (and Cs) speciate with chloride in the volcanic plume, forming aerosol. Arsenic, Re, Mo and Tl typically speciate with sulfur, oxygen or hydroxide.

well as Tl, commonly range between 50 and 100 % at other volcanoes (Fig. 9). The volatilities of chloride-speciating chalcophile and lithophile elements such as Cs, Cu, Zn, Ag, Sb are strongly linked to the Cl/S ratio of the volcanic gas (Fig. 9), suggesting that the availability of Cl (i.e. the salinity of the exsolved magmatic fluid) is a first order control on the emission of these elements in the gas phase.

4.3. Speciation of chalcophile elements in volcanic gases

Speciation modelling (Figs. 10 and 11) confirms the strong affinity that many of the chalcophile elements have for chloride in the gas phase. Copper concentrations in the aerosol phase are moderately high at Villarrica and other arc volcanoes due to the high abundance of Cl enhancing the volatility of Cu (Fig. 9), not because the melts are particularly enriched in Cu (Fig. 4). Caesium is both enriched in arc melts via the slab flux (Fig. 4) and in arc volcanic gases due to its chloride speciation (Fig. 9). Arsenic, in contrast, is enriched in arc melts via the slab flux (Fig. 4) but in arc volcanic gases the volatility of As overlaps with that of intraplate volcanic settings. Zelenski et al., (2021) calculate a higher fluid-melt partitioning for intraplate settings over arc settings; this is due to As speciating with sulfur rather than chloride (Figs. 10, 11), which is not enriched in arc volcanic gases. Similarly, Pb is enriched in arc melts due to slab flux (Fig. 4), but its volatility is similar in both arc and intraplate settings as it can speciate equally well with sulfur-bearing or chloride ligands in the gas phase (Fig. 11). Although not measured here, Se and Te are not enriched in arc melts over MORB (Jenner, 2017) but are likely equally volatile in both arc and intraplate volcanic settings, although more work is needed to confirm this.

Our results extend and are consistent with previous work emphasising the role of fluid salinity in modulating outgassed trace element assemblages. Zelenski et al. (2021) present a synthesis of volcanic gas and melt data to estimate fluid-melt partition coefficients for a range of trace metals, where elements with a fluid-melt partition coefficient of 1 or more are the volatile elements S and Cl, as well as Se, Te, Tl, Re, Bi, Cd, Au, In and As. The volatilities of chloride-speciating elements are enhanced in chlorine-rich arc systems (Zelenski et al., 2021). Further, experiments on Sn and Ag partitioning between felsic melts and aqueous fluids report fluid-melt partition coefficients of > 1, which increase with increasing salinity of the co-existing fluid (Simon et al., 2008; Yin and Zajacz, 2018; Zhao et al., 2022). Analysis of co-existing melt and fluid inclusions trapped in quartz in volatile-saturated systems suggest vapor-melt partition coefficients of > 1, and up to 30, for Cu, Ag, Zn, Pb, Bi, Mo, Sb, Sn, As and W, with the partition coefficients for Pb, Zn, Ag showing a linear increase with the salinity of the aqueous fluid suggesting these metals are transported as chloride complexes (Zajacz et al., 2008).

5. Conclusions

By combining geochemical data from melts and emitted volcanic gases at an open-vent arc system, we highlight the importance of both the fluid composition (i.e. salinity) and the melt composition (i.e. slab contributions, oxidation state) in modulating the behaviour of chalcophile elements in arc magmas and explaining the contrasting assemblages of outgassed trace elements observed between different tectonic settings. Experimental fluid-melt partition coefficients for chalcophile elements over a range of Cl contents and pressures for mafic melts are needed to constrain further the metal carrying-capacity of arc fluids from slab to surface, and at depths relevant to ore formation.

We show that melts erupted at Villarrica and other arc volcanoes are enriched (over mid-ocean ridge basalts) in a suite of fluid-mobile elements, including the chalcophile elements W, Tl, Pb and Sb. Volcanic gas and aerosol samples show that the chalcophile elements are strongly enriched in the gas phase over the silicate melt, 10^3 to 10^6 times more enriched than non-volatile REE. Volatilities reach ~45 % for Tl, with Pb, Sn and Mo exhibiting volatilities of up to 0.3 % and Cu up to 0.08 %. Many of the chalcophile elements (e.g. Cu, Ag, Zn) have an affinity for chloride in the gas phase and we observe that the volatility of chloride-speciating trace metals is linked strongly to the availability of chlorine in volcanic plumes globally.

Author contributions

EMM, EJN and KW carried out all the fieldwork with local assistance from GVV. EMM carried out the sample preparation, with assistance from EI and EJN. SH carried out the analysis of aerosol samples at the OU. EMM carried out data processing, and all authors contributed to interpretation of the data. Figure creation and manuscript drafting was led by EMM and ME, with assistance from all authors.

CRediT authorship contribution statement

Emily Mason: Data curation, Formal analysis, Investigation, Methodology, Validation, Visualization, Writing - original draft. **Marie Edmonds:** Conceptualization, Formal Analysis, Funding Acquisition, Investigation, Methodology, Project Administrtion, Supervision, Writing - original draft, Writing - review & editing. **Samantha Hammond:** Methodology, Formal analysis, Writing - review & editing. **Evgenia Ilyinskaya:** Methodology, Formal analysis, Supervision, Writing - review & editing. **Frances Jenner:** Methodology, Formal analysis, Supervision, Writing - review & editing. **Barbara Kunz:** Methodology, Formal analysis, Writing - review & editing. **Emma Nicholson:** Formal analysis, Investigation, Methodology, Validation, Visualization, Supervision, Writing - review & editing. **Gabriela Velasquez:** Methodology, Formal analysis, Investigation.

Declaration of competing interest

The authors declare that they have no known competing financial interests or personal relationships that could have appeared to influence the work reported in this paper.

Data availability

Data are available through the University of Cambridge at https://doi.org/10.17863/CAM.101999.

Acknowledgements

Thanks to Dr Iris Buisman at the University of Cambridge for assistance with EMPA analysis. Sincere thanks also to Coco and Richard from Sierra Nevada, our very patient and supportive guides during fieldwork at Villarrica. We are extremely grateful to OVDAS for their collaboration and for liaising with CONAF for access permissions on our behalf. This work was funded by an EPSRC postgraduate studentship to E.M, and a Leverhulme Early Career Fellowship to E.J.N. B.K. was supported by NERC grant 'From arc magmas to ore systems' (NE/P017045/1) held by F.J.

Appendix A. Supplementary material

Thanks to Dr Iris Buisman at the University of Cambridge for assistance with EMPA analysis. Sincere thanks also to Coco and Richard from Sierra Nevada, our very patient and supportive guides during fieldwork at Villarrica. We are extremely grateful to OVDAS for their collaboration and for liaising with CONAF for access permissions on our behalf. This work was funded by an EPSRC postgraduate studentship to E.M, and a Leverhulme Early Career Fellowship to E.J.N. B.K. was supported by NERC grant 'From arc magmas to ore systems' (NE/P017045/1) held by F.J. Supplementary material to this article can be found online at https://doi.org/10.1016/j.gca.2023.12.014.

References

Aiuppa, A., 2009. Degassing of halogens from basaltic volcanism: Insights from volcanic gas observations. Chem. Geol. 263, 99–109.

Aiuppa, A., Dongarrà, G., Valenza, M., Federico, C., Pecoraino, G., 2003. Degassing of trace volatile metals during the 2001 eruption of Etna. Volcanism Earth's Atmos. 41–54.

Aiuppa, A., Shinohara, H., Tamburello, G., Giudice, G., Liuzzo, M., Moretti, R., 2011. Hydrogen in the gas plume of an open-vent volcano, Mount Etna, Italy. J. Geophys. Res.: Solid Earth 116.

Aiuppa, A., Bitetto, M., Francofonte, V., Velasquez, G., Parra, C.B., Giudice, G., Liuzzo, M., Moretti, R., Moussallam, Y., Peters, N., 2017. A CO_2-gas precursor to the March 2015 Villarrica volcano eruption. Geochem. Geophys. Geosyst. 18, 2120–2132.

Allard, P., Aiuppa, A., Loyer, H., Carrot, F., Gaudry, A., Pinte, G., Michel, A., Dongarrà, G., 2000. Acid gas and metal emission rates during long-lived basalt degassing at Stromboli volcano. Geophys. Res. Lett. 27, 1207–1210.

Allard, P., Aiuppa, A., Bani, P., Métrich, N., Bertagnini, A., Gauthier, P.-J., Shinohara, H., Sawyer, G., Parello, F., Bagnato, E., 2016. Prodigious emission rates and magma degassing budget of major, trace and radioactive volatile species from Ambrym basaltic volcano, Vanuatu island Arc. J. Volcanol. Geoth. Res. 322, 119–143.

Allen, A.G., Baxter, P.J., Ottley, C.J., 2000. Gas and particle emissions from Soufrière Hills Volcano, Montserrat, West Indies: characterization and health hazard assessment. Bull. Volcanol. 62, 8–19.

Audétat, A., Zhang, L., Ni, H., 2018. Copper and Li diffusion in plagioclase, pyroxenes, olivine and apatite, and consequences for the composition of melt inclusions. Geochim. Cosmochim. Acta 243, 99–115.

Beermann, O., Botcharnikov, R., Holtz, F., Diedrich, O., Nowak, M., 2011. Temperature dependence of sulfide and sulfate solubility in olivine-saturated basaltic magmas. Geochim. Cosmochim. Acta 75, 7612–7631.

Blundy, J., Cashman, K., 2005. Rapid decompression-driven crystallization recorded by melt inclusions from Mount St. Helens Volcano. Geology 33, 793–796.

Buat-Ménard, P., Arnold, M., 1978. The heavy metal chemistry of atmospheric particulate matter emitted by Mount Etna Volcano. Geophys. Res. Lett. 5, 245–248.

Candela, P.A., 1997. A review of shallow, ore-related granites: textures, volatiles, and ore metals. J. Petrol. 38, 1619–1633.

Candela, P.A., Holland, H.D., 1984. The partitioning of copper and molybdenum between silicate melts and aqueous fluids. Geochim. Cosmochim. Acta 48, 373–380.

Chen, K., Tang, M., Lee, C.-T.-A., Wang, Z., Zou, Z., Hu, Z., Liu, Y., 2020. Sulfide-bearing cumulates in deep continental arcs: The missing copper reservoir. Earth Planet. Sci. Lett. 531, 115971.

Chiodini, G., Marini, L., 1998. Hydrothermal gas equilibria: the H_2O-H_2-CO_2-CO-CH_4 system. Geochim. Cosmochim. Acta 62, 2673–2687.

Cox, D., Watt, S.F., Jenner, F.E., Hastie, A.R., Hammond, S.J., 2019. Chalcophile element processing beneath a continental arc stratovolcano. Earth Planet. Sci. Lett. 522, 1–11.

Deschamps, F., Guillot, S., Godard, M., Andreani, M., Hattori, K., 2011. Serpentinites act as sponges for fluid-mobile elements in abyssal and subduction zone environments. Terra Nova 23, 171–178.

D'Souza, R.J., Canil, D., 2018. The partitioning of chalcophile elements between sediment melts and fluids at 3 GPa, 950–1050 °C with implications for slab fluids in subduction zones. Earth Planet. Sci. Lett. 498, 215–225.

Edmonds, M., Wallace, P.J., 2017. Volatiles and exsolved vapor in volcanic systems. Elements 13, 29–34.

Edmonds, M., Liu, E., Cashman, K., 2022. Open-vent volcanoes fuelled by depth-integrated magma degassing. Bull. Volcanol. 84, 1–27.

Edmonds, M., 2021. Geochemical monitoring of volcanoes and the mitigation of volcanic gas hazards. In: Forecasting and Planning for Volcanic Hazards, Risks, and Disasters. Elsevier, pp. 117-151.

Fischer, T.P., Chiodini, G., 2015. Volcanic, magmatic and hydrothermal gases. In: The encyclopedia of volcanoes. Elsevier, pp. 779-797.

Gauthier, P.J., Sigmarsson, O., Gouhier, M., Haddadi, B., Moune, S., 2016. Elevated gas flux and trace metal degassing from the 2014–2015 fissure eruption at the Bárðarbunga volcanic system, Iceland. J. Geophys. Res. Solid Earth 121, 1610–1630.

Gerlach, T., 2004. Volcanic sources of tropospheric ozone-depleting trace gases. Geochem. Geophys. Geosyst. 5, Q09007.

Giggenbach, W., 1996. Chemical composition of volcanic gases. In: Monitoring and mitigation of volcano hazards. Springer, pp. 221-256.

Grondahl, C., Zajacz, Z., 2022. Sulfur and chlorine budgets control the ore fertility of arc magmas. Nat. Commun. 13, 4218.

Hedenquist, J.W., Lowenstern, J.B., 1994. The role of magmas in the formation of hydrothermal ore deposits. Nature 370, 519–527.

Heinrich, C., Günther, D., Audétat, A., Ulrich, T., Frischknecht, R., 1999. Metal fractionation between magmatic brine and vapor, determined by microanalysis of fluid inclusions. Geology 27, 755–758.

Heinrich, C.A., Ryan, C.G., Mernagh, T.P., Eadington, P.J., 1992. Segregation of ore metals between magmatic brine and vapor; a fluid inclusion study using PIXE microanalysis. Econ. Geol. 87, 1566–1583.

Hinkley, T.K., 1991. Distribution of metals between particulate and gaseous forms in a volcanic plume. Bull. Volcanol. 53, 395–400.

Hinkley, T.K., Lamothe, P.J., Wilson, S.A., Finnegan, D.L., Gerlach, T.M., 1999. Metal emissions from Kilauea, and a suggested revision of the estimated worldwide metal output by quiescent degassing of volcanoes. Earth Planet. Sci. Lett. 170, 315–325.

Ilyinskaya, E., Schmidt, A., Mather, T.A., Pope, F.D., Witham, C., Baxter, P., Jóhannsson, T., Pfeffer, M., Barsotti, S., Singh, A., 2017. Understanding the environmental impacts of large fissure eruptions: Aerosol and gas emissions from the 2014–2015 Holuhraun eruption (Iceland). Earth Planet. Sci. Lett. 472, 309–322.

Ilyinskaya, E., Mason, E., Wieser, P.E., Holland, L., Liu, E.J., Mather, T.A., Edmonds, M., Whitty, R.C., Elias, T., Nadeau, P.A., 2021. Rapid metal pollutant deposition from the volcanic plume of Kīlauea, Hawai'i. Commun. Earth Environ. 2, 1–15.

Jenner, F.E., 2017. Cumulate causes for the low contents of sulfide-loving elements in the continental crust. Nat. Geosci. 10, 524.

Jenner, F.E., O'Neill, H.S., 2012. Analysis of 60 elements in 616 ocean floor basaltic glasses. Geochem. Geophys. Geosyst. 13 (2).

Johnson, J.B., Watson, L.M., Palma, J.L., Dunham, E.M., Anderson, J.F., 2018. Forecasting the eruption of an open-vent volcano using resonant infrasound tones. Geophys. Res. Lett. 45, 2213–2220.

Jugo, P.J., 2009. Sulfur content at sulfide saturation in oxidized magmas. Geology 37, 415–418.

Keppler, H., Wyllie, P.J., 1991. Partitioning of Cu, Sn, Mo, W, U, and Th between melt and aqueous fluid in the systems haplogranite-H_2O− HCl and haplogranite-H_2O− HF. Contr. Mineral. and Petrol. 109, 139–150.

Kiseeva, E.S., Wood, B.J., 2013. A simple model for chalcophile element partitioning between sulphide and silicate liquids with geochemical applications. Earth Planet. Sci. Lett. 383, 68–81.

Lambert, G., Le Cloarec, M., Ardouin, B., Le Roulley, J., 1985. Volcanic emission of radionuclides and magma dynamics. Earth Planet. Sci. Lett. 76, 185–192.

Lee, C.-T.-A., Tang, M., 2020. How to make porphyry copper deposits. Earth Planet. Sci. Lett. 529, 115868.

Liu, E.J., Wood, K., Mason, E., Edmonds, M., Aiuppa, A., Giudice, G., Bitetto, M., Francofonte, V., Burrow, S., Richardson, T., 2019. Dynamics of outgassing and plume transport revealed by proximal Unmanned Aerial System (UAS) measurements at Volcán Villarrica, Chile. Geochem. Geophys. Geosyst. 20, 730–750.

Mandon, C.L., Christenson, B.W., Schipper, C.I., Seward, T.M., Garaebiti, E.J.J.O.V., 2019. Metal transport in volcanic plumes: a case study at White Island and Yasur volcanoes. J. Volcanol. Geoth. Res. 369, 155–171.

Mandon, C.L., Seward, T.M., Christenson, B.W., 2020. Volatile transport of metals and the Cu budget of the active White Island magmatic-hydrothermal system, New Zealand. J. Volcanol. Geoth. Res. 398, 106905.

Martin, R., Mather, T., Pyle, D., 2006. High-temperature mixtures of magmatic and atmospheric gases. Geochem. Geophys. Geosyst. 7.

Mason, E., Wieser, P.E., Liu, E.J., Edmonds, M., Ilyinskaya, E., Whitty, R.C., Mather, T.A., Elias, T., Nadeau, P.A., Wilkes, T.C., 2021. Volatile metal emissions from volcanic degassing and lava–seawater interactions at Kīlauea Volcano, Hawai'i. Commun. Earth Environ. 2, 1–16.

Mason, E., 2021. Volatile metal degassing from volcanoes: source processes, atmospheric transport and deposition. PhD University of Cambridge.

Mather, T., Pyle, D., Oppenheimer, C., 2003. Tropospheric volcanic aerosol. In: Volcanism and the Earth's Atmosphere. American Geophysical Union, Geophysical Monograph. pp. 189-212.

Mather, T., Tsanev, V., Pyle, D., McGonigle, A., Oppenheimer, C., Allen, A., 2004. Characterization and evolution of tropospheric plumes from Lascar and Villarrica volcanoes, Chile. J. Geophys. Res.: Atmos. 109.

Mather, T.A., Witt, M.L.I., Pyle, D.M., Quayle, B.M., Aiuppa, A., Bagnato, E., Martin, R.S., Sims, K.W.W., Edmonds, M., Sutton, A.J., Ilyinskaya, E., 2012. Halogens and trace metal emissions from the ongoing 2008 summit eruption of Kīlauea volcano, Hawai'i. Geochim. Cosmochim. Acta 83, 292–323.

Moretti, R., Papale, P., Ottonello, G., 2003. A model for the saturation of COHS fluids in silicate melts. Geol. Soc. Lond. Spec. Publ. 213, 81–101.

Moune, S., Gauthier, P.-J., Delmelle, P., 2010. Trace elements in the particulate phase of the plume of Masaya Volcano, Nicaragua. J. Volcanol. Geoth. Res. 193, 232–244.

Moussallam, Y., Bani, P., Curtis, A., Barnie, T., Moussallam, M., Peters, N., Schipper, C.I., Aiuppa, A., Giudice, G., Amigo, Á., 2016. Sustaining persistent lava lakes: Observations from high-resolution gas measurements at Villarrica volcano, Chile. Earth Planet. Sci. Lett. 454, 237–247.

Moussallam, Y., Oppenheimer, C., Scaillet, B., 2019. On the relationship between oxidation state and temperature of volcanic gas emissions. Earth Planet. Sci. Lett. 520, 260–267.

Mungall, J.E., Brenan, J.M., Godel, B., Barnes, S., Gaillard, F., 2015. Transport of metals and sulphur in magmas by flotation of sulphide melt on vapour bubbles. Nat. Geosci. 8, 216–219.

Nielsen, S.G., Prytulak, J., Blusztajn, J., Shu, Y., Auro, M., Regelous, M., Walker, J., 2017. Thallium isotopes as tracers of recycled materials in subduction zones: Review and new data for lavas from Tonga-Kermadec and Central America. J. Volcanol. Geoth. Res. 339, 23–40.

Noll Jr, P., Newsom, H., Leeman, W., Ryan, J.G., 1996. The role of hydrothermal fluids in the production of subduction zone magmas: evidence from siderophile and chalcophile trace elements and boron. Geochim. Cosmochim. Acta 60, 587–611.

O'Neill, H.S., Mavrogenes, J.A., 2022. The sulfate capacities of silicate melts. Geochim. Cosmochim. Acta 334, 368–382.

Palma, J.L., Calder, E.S., Basualto, D., Blake, S., Rothery, D.A., 2008. Correlations between SO_2 flux, seismicity, and outgassing activity at the open vent of Villarrica volcano, Chile. J. Geophys. Res.: Solid Earth 113.

Patten, C., Barnes, S.-J., Mathez, E.A., Jenner, F.E., 2013. Partition coefficients of chalcophile elements between sulfide and silicate melts and the early crystallization history of sulfide liquid: LA-ICP-MS analysis of MORB sulfide droplets. Chem. Geol. 358, 170–188.

Pioli, L., Scalisi, L., Costantini, L., Di Muro, A., Bonadonna, C., Clavero, J., 2015. Explosive style, magma degassing and evolution in the Chaimilla eruption, Villarrica volcano, Southern Andes. Bull. Volcanol. 77, 1–14.

Reekie, C., Jenner, F., Smythe, D., Hauri, E., Bullock, E., Williams, H., 2019. Sulfide resorption during crustal ascent and degassing of oceanic plateau basalts. Nat. Commun. 10, 82.
Rezeau, H., Jagoutz, O., 2020. The importance of H_2O in arc magmas for the formation of porphyry Cu deposits. Ore Geol. Rev. 126, 103744.
Richards, J.P., 2015. The oxidation state, and sulfur and Cu contents of arc magmas: implications for metallogeny. Lithos 233, 27–45.
Romero, J.E., Vera, F., Polacci, M., Morgavi, D., Arzilli, F., Alam, M.A., Bustillos, J.E., Guevara, A., Johnson, J.B., Palma, J.L., 2018. Tephra from the 3 March 2015 sustained column related to explosive lava fountain activity at Volcán Villarrica (Chile). Front. Earth Sci. 6, 98.
Rudnick, R., Gao, S., 2003. Composition of the Continental crust. Treatise Geochem. 3, 1–64.
Sawyer, G.M., Salerno, G.G., Le Blond, J.S., Martin, R.S., Spampinato, L., Roberts, T.J., Mather, T.A., Witt, M.L.I., Tsanev, V.I., Oppenheimer, C., 2011. Gas and aerosol emissions from Villarrica volcano, Chile. J. Volcanol. Geoth. Res. 203, 62–75.
Shaw, D.M., 1952. The geochemistry of thallium. Geochim. Cosmochim. Acta 2, 118–154.
Shinohara, H., Witter, J., 2005. Volcanic gases emitted during mild Strombolian activity of Villarrica volcano, Chile. Geophys. Res. Lett. 32.
Sillitoe, R.H., 2010. Porphyry copper systems. Econ. Geol. 105, 3–41.
Simon, A.C., Pettke, T., Candela, P.A., Piccoli, P.M., 2008. The partitioning behavior of silver in a vapor–brine–rhyolite melt assemblage. Geochim. Cosmochim. Acta 72, 1638–1659.
Smythe, D.J., Wood, B.J., Kiseeva, E.S., 2017. The S content of silicate melts at sulfide saturation: new experiments and a model incorporating the effects of sulfide composition. Am. Mineral. 102, 795–803.
Stewart, C., Damby, D.E., Horwell, C.J., Elias, T., Ilyinskaya, E., Tomašek, I., Longo, B.M., Schmidt, A., Carlsen, H.K., Mason, E., 2022. Volcanic air pollution and human health: recent advances and future directions. Bull. Volcanol. 84, 11.
Symonds, R.B., Rose, W.I., Bluth, G.J., Gerlach, T.M., 1994. Volcanic-gas studies; methods, results, and applications. Rev. Mineral. Geochem. 30, 1–66.
Turner, S.J., Langmuir, C.H., 2015. The global chemical systematics of arc front stratovolcanoes: Evaluating the role of crustal processes. Earth Planet. Sci. Lett. 422, 182–193.
Walters, J.B., Cruz-Uribe, A.M., Marschall, H.R., Boucher, B., 2021. The role of sulfides in the chalcophile and siderophile element budget of the subducted oceanic crust. Geochim. Cosmochim. Acta 304, 191–215.
Whitby, K.T., 1978. The physical characteristics of sulfur aerosols. In: Sulfur in the Atmosphere. Elsevier, pp. 135-159.
Wieser, P.E., Jenner, F., Edmonds, M., Maclennan, J., Kunz, B.E., 2020. Chalcophile elements track the fate of sulfur at Kīlauea Volcano, Hawai'i. Geochim. Cosmochim. Acta 282, 245–275.
Williams-Jones, A.E., Heinrich, C.A., 2005. 100th Anniversary special paper: vapor transport of metals and the formation of magmatic-hydrothermal ore deposits. Econ. Geol. 100, 1287–1312.
Witter, J.B., Kress, V.C., Delmelle, P., Stix, J., 2004. Volatile degassing, petrology, and magma dynamics of the Villarrica Lava Lake, Southern Chile. J. Volcanol. Geoth. Res. 134, 303–337.
Wu, K., Yuan, H., Lyu, N., Zhang, L., 2020. The behavior of fluid mobile elements during serpentinization and dehydration of serpentinites in subduction zones. Acta Petrol. Sin. 36, 141–153.
Yin, Y., Zajacz, Z., 2018. The solubility of silver in magmatic fluids: Implications for silver transfer to the magmatic-hydrothermal ore-forming environment. Geochim. Cosmochim. Acta 238, 235–251.
Zajacz, Z., Halter, W., 2009. Copper transport by high temperature, sulfur-rich magmatic vapor: Evidence from silicate melt and vapor inclusions in a basaltic andesite from the Villarrica volcano (Chile). Earth Planet. Sci. Lett. 282, 115–121.
Zajacz, Z., Halter, W.E., Pettke, T., Guillong, M., 2008. Determination of fluid/melt partition coefficients by LA-ICPMS analysis of co-existing fluid and silicate melt inclusions: controls on element partitioning. Geochim. Cosmochim. Acta 72, 2169–2197.
Zelenski, M.E., Fischer, T.P., de Moor, J.M., Marty, B., Zimmermann, L., Ayalew, D., Nekrasov, A.N., Karandashev, V.K., 2013. Trace elements in the gas emissions from the Erta Ale volcano, Afar, Ethiopia. Chem. Geol. 357, 95–116.
Zelenski, M., Malik, N., Taran, Y., 2014. Emissions of trace elements during the 2012–2013 effusive eruption of Tolbachik volcano, Kamchatka: enrichment factors, partition coefficients and aerosol contribution. J. Volcanol. Geoth. Res. 285, 136–149.
Zelenski, M., Simakin, A., Taran, Y., Kamenetsky, V., Malik, N.J., 2021. Partitioning of elements between high-temperature, low-density aqueous fluid and silicate melt as derived from volcanic gas geochemistry. Geochim. Cosmochim. Acta 295, 112–134.
Zhao, P., Zajacz, Z., Tsay, A., Yuan, S., 2022. Magmatic-hydrothermal tin deposits form in response to efficient tin extraction upon magma degassing. Geochim. Cosmochim. Acta 316, 331–346.